

SPACE DEBRIS: A GROWING PROBLEM

A Thesis Submitted in Partial Satisfaction  
Of the Requirements for the Degree of  
Bachelor of Science in Physics  
at the  
University of California, Santa Cruz

By  
Michael B. Rosenberg  
June 1, 2010

---

David P. Belanger  
Advisor

---

David P. Belanger  
Senior Theses Coordinator

---

David P. Belanger  
Chair, Department of Physics

## **Abstract**

The large amount of space debris in the LEO region poses a constantly increasing threat to our satellites and future space-based missions of all kinds. The purpose of this thesis is to analyze the growth in the amount of debris within the region of space between 200km and 2000km, and to make a projection of future levels of debris density. I will be documenting the overall distribution of the debris and how that affects current and future satellites.

## **Materials**

- Desktop Computer for running ORDEM
- Ordem2000, Modeling software
- UCS (Union of Concerned Scientists) Satellite Database
- Excel

## **List of Tables**

**Table 1:** Latitude = 80, Observation Year = 2008

**Table 2:** Shows the first 1/8 of the debris data from the year 2000 in the 200-400km region.

**Table 3:** The averaged version of table 1, it also has the standard deviation from the average

**Table 4:** The average data from 2000-2008 for the 10 $\mu$ m data, including the error and 3 highlighted sections that will be graphed for in-depth analysis.

**Table 5:** The 10 $\mu$ m debris trend shortened into 5 year snapshots, it includes the percent increase in density from the year 2000 to the year 2030, as well as the goodness of fit value for the measurement of how well the data fit a linear approximation.

**Table 6:** The 100 $\mu$ m debris trend shortened into 5-year snapshots, it includes the percent increase in density from the year 2000 to the year 2030, as well as the goodness of fit value for the measurement of how well the data fit a linear approximation.

**Table 7:** The 1mm debris trend shortened into 5-year snapshots, it includes the percent increase in density from the year 2000 to the year 2030, as well as the goodness of fit value for the measurement of how well the data fit a linear approximation.

**Table 8:** The 1cm debris trend shortened into 5 year snapshots, it includes the percent increase in density from the year 2000 to the year 2030, as well as the goodness of fit value for the measurement of how well the data fit a linear approximation.

**Table 9:** The 10cm debris trend shortened into 5 year snapshots, it includes the percent increase in density from the year 2000 to the year 2030, as well as the goodness of fit value for the measurement of how well the data fit a linear approximation.

**Table 10:** The 1m debris trend shortened into 5 year snapshots, it includes the percent increase in density from the year 2000 to the year 2030, as well as the goodness of fit value for the measurement of how well the data fit a linear approximation.

**Table 11:** The complete set of data from 2009 to 2030 for 10 $\mu$ m and 100 $\mu$ m.

**Table 12:** The complete set of data from 2009 to 2030 for 1mm and 1cm.

**Table 13:** The complete set of data from 2009 to 2030 for 10cm and 1m.

**Table 14:** The percent increase and goodness of fit for

### **List of Figures**

**Figure 1:** Density in the year 2008 from 200km to 500km and 19 latitudes of interest.

**Figure 2:** Density in the year 2008 from 550km to 850km and 19 latitudes of interest.

**Figure 3:** Density in the year 2008 from 850km to 1150km and 19 latitudes of interest.

**Figure 4:** Density in the year 2008 from 1200km to 1500km and 19 latitudes of interest.

**Figure 5:** Density in the year 2008 from 1550km to 1950km and 19 latitudes of interest.

**Figure 6:** Density at 400km of the 10 $\mu$ m and larger objects averaged over 19 latitudes from the year 2000-2008.

**Figure 7:** Density at 800km of the 10 $\mu$ m and larger objects averaged over 19 latitudes from the year 2000-2008.

**Figure 8:** Density at 1200km of the 10 $\mu$ m and larger objects averaged over 19 latitudes from the year 2000-2008.

**Figure 9:** Density of the 10 $\mu$ m objects in 2008 vs 2030.

**Figure 10:** Density of the 100 $\mu$ m objects in 2008 vs 2030.

**Figure 11:** Density of the 1mm objects in 2008 vs 2030.

**Figure 12:** Density of the 1m objects in 2008 vs 2030.

## **Introduction**

Earth orbits are separated into 3 groups. The first group is HEO (High Earth Orbit) and it is located at or above 36,000km. The next region is MED (Middle Earth Orbit) which is located between 2000km and 36,000km. The lowest region of space is the LEO (Low Earth Orbit), which is the region of space below 2000km. The LEO contains about 1/3 of the total number of active satellites today, most of the rest can be found in the GEO (geosynchronous earth orbit) near HEO<sup>1</sup>. GEO is an orbit that rotates around the earth at the same speed the earth rotates.

Most of our modern communication satellites which we rely on for things like satellite television are located in GEO at around 35,786km, and have an orbital velocity of about 3.07km/s.<sup>2</sup> This allows them to stay stationary relative to the ground while operating. A large

---

<sup>1</sup> UCS satellite database

<sup>2</sup> [http://www.centennialofflight.gov/essay/Dictionary/GEO\\_ORBIT/DI146.html](http://www.centennialofflight.gov/essay/Dictionary/GEO_ORBIT/DI146.html)

earth-based antenna can point in a fixed direction to maintain a strong connection to the satellite. The risk of debris and collisions is also much smaller for several reasons at HEO.

The first reason is that all the satellites in this region are relatively stationary with respect to the ground they orbit over, which implies that they will all be just as stationary with respect to each other. The velocity of each satellite is also much lower than LEO because the high orbital altitude requires a much lower speed to stay in orbit. Most of the debris that comes from things multi-stage boosting rockets either gets trapped in LEO or travels past HEO and does not return. Any debris that is caused in GEO will tend to travel with the satellites instead of against them.<sup>3</sup>

LEO satellites are much different from their HEO counterparts. Since they cannot maintain a GEO and need to travel much faster, they completely circle the earth many times in a single day. The average satellite in LEO moves at around 8km/s and they don't all orbit in the same direction like the GEO satellites do<sup>4</sup>. Some LEO satellites have polar orbits, some stay with the equator, some do neither. The debris located in LEO travels at these high velocities with many diverse types of orbits.

Around 12 percent of the total space debris population are objects involved in normal satellite deployment. Objects in this category include fasteners, nozzle covers, lens caps, straps, and multiple payload mechanisms. Another large contributor of space debris is the slag from solid rocket motors. The fragmentation of the upper stages of satellites and spacecraft accounts for around 43 percent of all the current identified space debris. The vast majority of objects larger than 5cm are from this source.

In orbit explosions account for about 36% of space object breakups. Accidental explosions happen to both currently in operating and abandoned satellites. Malfunctioning

---

<sup>3</sup> [http://orbitaldebris.jsc.nasa.gov/library/UN\\_Report\\_on\\_Space\\_Debris99.pdf](http://orbitaldebris.jsc.nasa.gov/library/UN_Report_on_Space_Debris99.pdf) page 28

<sup>4</sup> [http://orbitaldebris.jsc.nasa.gov/library/UN\\_Report\\_on\\_Space\\_Debris99.pdf](http://orbitaldebris.jsc.nasa.gov/library/UN_Report_on_Space_Debris99.pdf) page 32

propulsion systems can fail catastrophically. Batteries can overcharge from solar panels and rupture.<sup>5</sup> At one time the United States and Russia had both done tests with what are known as anti-satellite weaponry. This was halted in the early 1980s and the Current United Nations policy strongly discourages such testing due to the impact it has on the LEO region. On January 11<sup>th</sup> 2007, the Fenyun-1C Chinese weather satellite was intentionally detonated with an anti satellite weapon. This 960km satellite was orbiting at 865km when the missile test was conducted. The result is the single largest pollution of LEO in the past 50 years. Due to the relatively recent nature of this event I was unable to include it in the predictions. However it's still worth mentioning because it will only help fuel the problems this thesis covers.<sup>6</sup>

Satellite cell phones are a good example of why LEO satellites are necessary. A phone does not have a large directional antenna and it can't broadcast to 36,000km by itself. Instead they must rely on LEO safelight clusters to function. Satellites that take pictures of the earth, either for science or espionage, need to move over a variety of positions on the globe. GEO would only allow them to take pictures of one general area, also it is much harder to take photos at that altitude due to the great distances involved. The LEO region is invaluable, and this is why it's the focus of this thesis.

## **Debris**

It is very difficult to put a number on the space debris density. There are several reasons for this. The first reason is that as the altitude changes, so does the density. However it is not just altitude that causes variability in density numbers, it is also the locations of the debris in *latitude* and *longitude*. These conceptual graphs are taken from the 100um object densities in the year 2008. It's important to understand where the space debris are located, and why they are there.

---

<sup>5</sup> [http://orbitaldebris.jsc.nasa.gov/library/UN\\_Report\\_on\\_Space\\_Debris99.pdf](http://orbitaldebris.jsc.nasa.gov/library/UN_Report_on_Space_Debris99.pdf) page 32

<sup>6</sup> <http://orbitaldebris.jsc.nasa.gov/newsletter/pdfs/ODQNV11i2.pdf> page 2

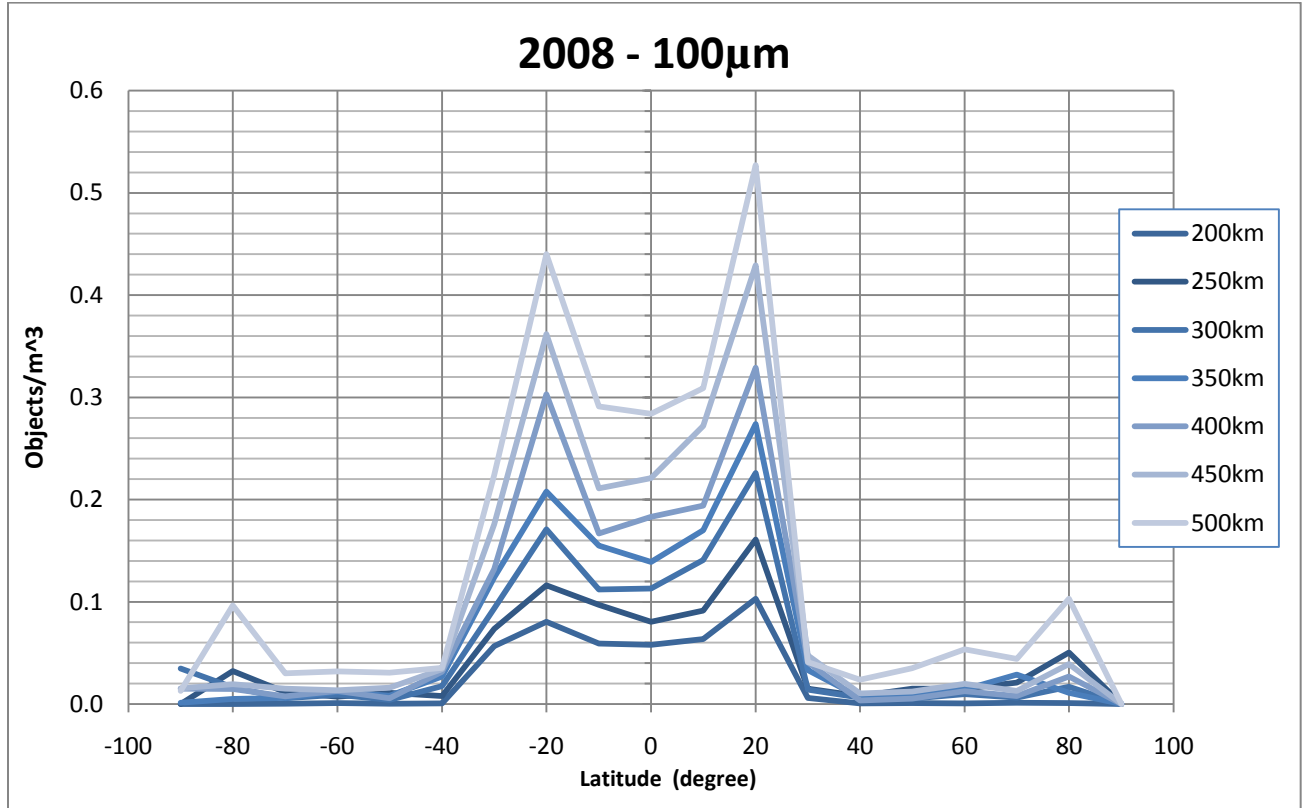


Figure 1 Density of 100µm objects/m<sup>3</sup> from 200km to 500km in 2008 at multiple latitudes. Nearly all the debris is crusted near the equator.

This first graph shows the density in objects/m<sup>3</sup> from 200km to 500km. These data points are taken every 10 degrees of latitude. Starting with 90 being directly above the North Pole, 0 being the equator, and -90 referring to the South Pole. If this graph was wrapped along the earth from top to bottom, and then projected around 360 degrees, it would be the 3 dimensional distribution of debris.

There is a much larger concentration near the equator than at the poles. However it does not peak in the middle, instead it has 2 maxima around 20 and -20. At 200km the peaks are low with respect to the middle so it does appear to have general maxima around the equator at 200km.

When I looked at higher altitudes this did not stay the same. As the altitude approaches 500km it becomes obvious that the peaks are significant. The local minimum between the 2 peaks is .3 objects per cubic meter at 500km, and the peaks reach up to .44 and .53. If we look closely at the 500km line, we can see two distinct small peaks developing near the +/- 80 mark. It is difficult to see the significance of this by only looking at the 500km graph. My next range of attitudes is from 550km to 850km. In this graph, the +/- 20 humps still exists, but they are joined be 2 more local maxima, one on each side at +/-80.

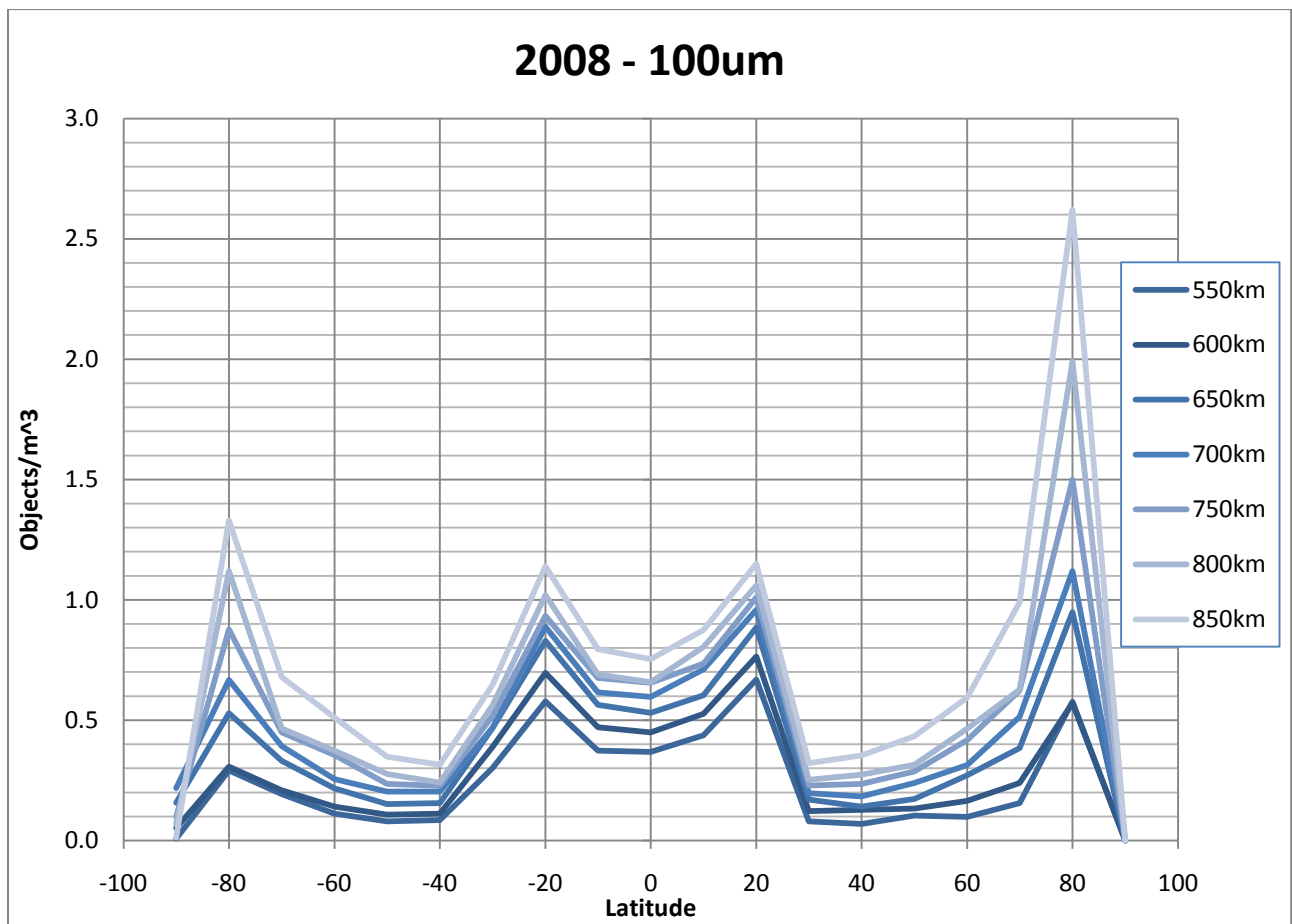


Figure 2 Density of 100µm objects/m³ from 550km to 850km in 2008 at multiple latitudes. Debris is clustered near the equator and near the poles.



By 950km, the +/-80 peaks in density are actually larger than the ones located near the equator. In order to explain these 4 peaks properly, I need to better describe what the graph and data are portraying.

Ordem2000 is averaging over longitudinal rings in the sky. The debris at and near the equator are located in a large ring around the planet. The debris near the North Pole and South Pole 80 degree mark are smaller clusters that sit above and below the planet. This means that each peak at +/-80 is actually two peaks, one at +/-80, and the other at +/-110. The equatorial peaks form a ring around the planet, while the polar peaks indicated something slightly different. If the polar density peaks were caused by a vertical ring of debris, we would expect to see higher densities in the +/- 40 to 70 range because the ring would pass through this area. The data are showing that the debris only become thicker near the poles. It's impossible for something to orbit just the North Pole, however. The orbit that best explains this is that there are many groups of debris in unique polar orbits that are intersecting near the poles. Polar orbits are more common at higher altitudes, so it makes sense that the +/- 80 degree peaks did not appear initially.

The next group is from 900 to 1200. The trend of the debris rings that cross near the poles continues to increase. In this altitude range the equatorial grouping of debris has actually become the less dominant group. This might be an indication that polar orbits are more common at these altitudes than equatorial orbits. The 1250 to 1550 range is nearly identical to the 900 to 1200 range as you can see below.

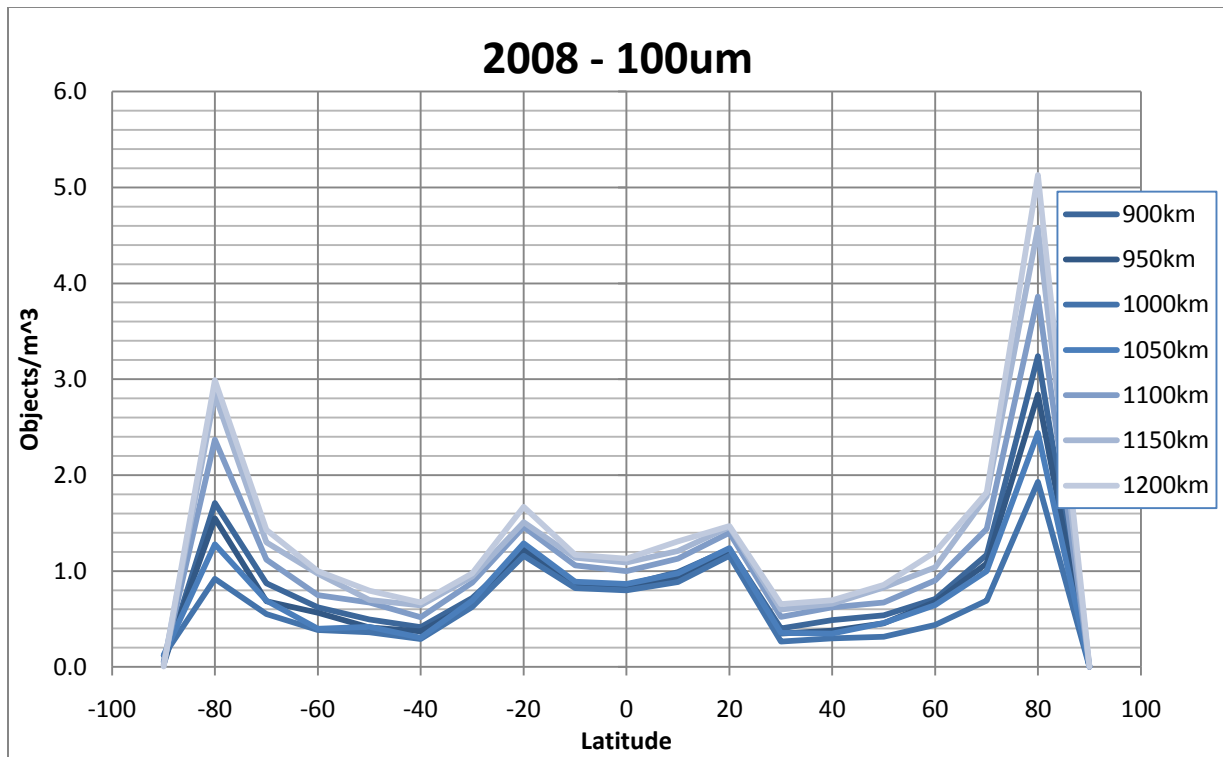


Figure 3 Density of 100µm objects/m<sup>3</sup> from 900km to 1200km in 2008 at multiple latitudes. Debris is clustered more near the poles than the equator.

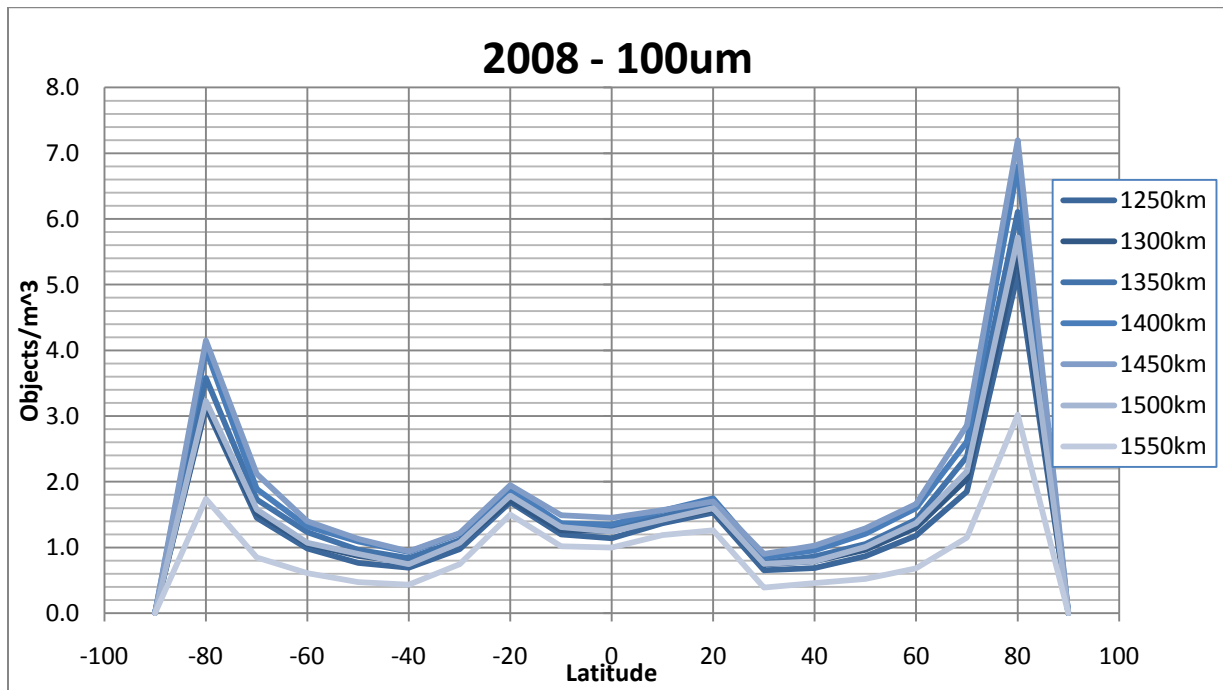


Figure 4 Density of 100µm objects/m<sup>3</sup> from 1250km to 1550km in 2008 at multiple latitudes. Debris is clustered more near the poles than the equator.

This reign of space from 850 to about 1500 is going to be combined into the 3<sup>rd</sup> group of LEO space. Unlike the first 2 regions, the density is decreasing as the altitude increases. The polar peaks are decreasing the fastest, and by 1600km they are nearly the same magnitude as the equatorial peak.

The final reign is from 1600km to 2000km; it's the farthest reaches of the LEO orbital space and has much lower densities of both satellites and debris.

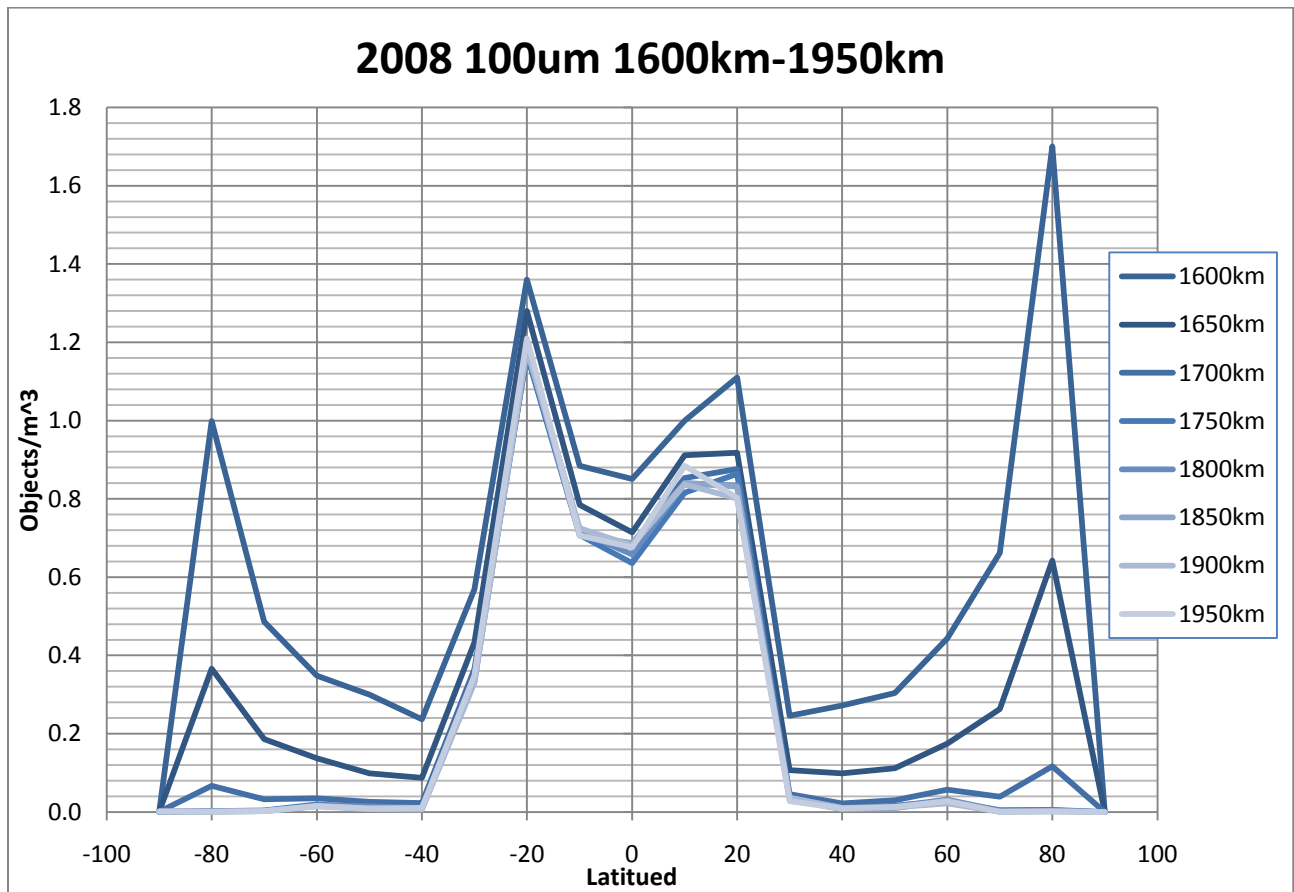


Figure 3 Density of 100µm objects/m<sup>3</sup> from 1600km to 1950km in 2008 at multiple latitudes. Debris cluster tends towards the equator as the altitude increases.

Past 1600km, the polar regions no longer dominate the graph. The reason we continue to see a grouping of debris at the equator is because the GEO satellites and other space missions travel through this region of space on the way to their destinations.

## Calculations

This presentation of debris data are created by an application known as ORDEM2000, which stands for Orbital Debris Engineering Model. It incorporates observation data from both space and ground-based observations covering an object size range from 10 u, to 1m. The program does not output an average density at a particular altitude, but instead it uses a specific latitude above the earth. In order to calculate a rate of growth for the debris size I needed to simplify this varying density into an average density.

Since I had studied the distribution of the density, I knew that it would not be appropriate to just focus on one particular latitude such as the equator. Instead I took data from every 10 degrees starting at the North Pole and ending at the South Pole. This gives me 19 data points to average over.

Latitude = 80, Observation Year = 2008

altitude	size>=10um	size>=100um	size>=1mm	size>=1cm	size>=10cm	size>=1m
200	9.32E-02	1.40E-04	2.33E-07	4.25E-10	4.25E-10	2.35E-10
250	2.91E-01	3.22E-02	3.28E-06	3.56E-10	3.56E-10	1.04E-10
300	3.14E-01	1.64E-02	1.60E-05	5.37E-09	1.05E-09	5.45E-10
350	7.66E-01	5.17E-03	1.60E-05	1.95E-08	2.06E-09	7.07E-10
400	9.74E-01	1.48E-02	2.94E-05	3.22E-08	4.01E-09	1.52E-09
450	2.72E+00	1.94E-02	4.75E-05	8.70E-08	8.17E-09	4.45E-09
500	2.44E+00	9.65E-02	9.52E-05	7.52E-08	1.37E-08	6.36E-09
550	4.08E+00	2.91E-01	1.85E-04	9.15E-08	1.75E-08	5.94E-09
600	5.93E+00	3.07E-01	2.15E-04	1.26E-07	2.25E-08	1.12E-08
650	7.69E+00	5.29E-01	3.04E-04	1.40E-07	1.72E-08	4.78E-09
700	9.54E+00	6.68E-01	4.04E-04	2.05E-07	1.98E-08	5.92E-09
750	1.05E+01	8.78E-01	5.84E-04	3.58E-07	3.11E-08	1.23E-08
800	1.22E+01	1.12E+00	3.90E-04	5.13E-07	3.41E-08	1.24E-08
850	1.32E+01	1.33E+00	2.04E-04	4.80E-07	3.26E-08	1.07E-08
900	1.41E+01	1.71E+00	1.76E-04	2.22E-07	3.54E-08	9.11E-09
950	1.55E+01	1.55E+00	3.78E-04	2.59E-07	5.59E-08	2.74E-08
1000	1.61E+01	9.17E-01	5.91E-04	2.10E-07	3.45E-08	8.88E-09
1050	1.78E+01	1.28E+00	6.00E-04	1.36E-07	2.41E-08	4.54E-09
1100	2.03E+01	2.37E+00	6.55E-04	1.26E-07	1.54E-08	2.83E-09
1150	2.09E+01	2.84E+00	6.17E-04	1.22E-07	1.15E-08	3.23E-09
1200	2.10E+01	2.99E+00	6.57E-04	1.42E-07	8.83E-09	1.80E-09
1250	2.03E+01	3.13E+00	8.55E-04	2.30E-07	1.22E-08	2.13E-09
1300	1.96E+01	3.18E+00	9.87E-04	2.91E-07	9.60E-09	1.39E-09
1350	1.95E+01	3.58E+00	1.06E-03	2.67E-07	1.54E-08	4.78E-09
1400	1.97E+01	4.01E+00	1.12E-03	2.39E-07	3.28E-08	1.69E-08
1450	2.15E+01	4.15E+00	9.85E-04	1.69E-07	2.06E-08	3.72E-09
1500	1.65E+01	3.23E+00	8.27E-04	1.31E-07	1.93E-08	3.26E-09
1550	1.25E+01	1.74E+00	5.25E-04	7.41E-08	9.01E-09	7.63E-10
1600	1.03E+01	9.99E-01	3.66E-04	4.55E-08	6.08E-09	6.85E-10
1650	7.79E+00	3.66E-01	2.42E-04	7.40E-08	5.41E-09	1.17E-09
1700	6.14E+00	6.65E-02	1.07E-04	8.45E-08	3.16E-09	5.16E-10
1750	4.74E+00	2.63E-03	1.71E-05	5.62E-08	2.40E-09	3.98E-10
1800	3.75E+00	1.70E-03	1.01E-05	2.84E-08	1.83E-09	2.82E-10
1850	2.94E+00	1.12E-03	7.84E-06	2.61E-08	1.63E-09	2.91E-10
1900	2.00E+00	2.99E-04	3.81E-06	2.49E-08	1.16E-09	1.22E-10
1950	1.58E+00	6.04E-04	4.83E-06	2.22E-08	9.56E-10	1.25E-10

Table 1 Data from ORDEM for the year 2008 at 80 degree latitude.

This is just one of the 19 data tables from the year 2008. I used 8 years of data which means in total I have 152 tables like the one above. Each table has a calculation of the number of objects per cubic meter of volume (the density of the debris). The density is broken down into 36 altitudes ranging from 200km to 1950km, and separated into 6 size groupings. This information I will use to calculate a rough rate of change in the density of debris.

The first decision is how to combine the 19 measurements into one average density for that altitude. Originally I assumed that focusing on the equator would give the most consistent results. However once I closely observed of the debris density changes with respect to latitude, I realized that any average based on the equator would not be appropriate. This, and the fact that I'm only looking for a relative increase between the years, lead me to doing an average across all 19 data points

$$\sum_0^9 ((X_+^0) + (X_-^0) - (0_-^0))/19 = D_{yA}$$

$D_{yA}$  is the overall density (D) for a given year (y) at a particular altitude (A). The error I am using is the standard deviation. The last term ( $0_-^0$ ) in both equation is just to deal with the fact that there is only one zero degree measurement

$$\sqrt{\frac{\sum_0^9 ((X_+^0 - D_{yA})^2 + (X_-^0 - D_{yA})^2 - (0_-^0 - D_{yA})^2)}{19}} = \sigma_{yA}$$

The standard deviation shows the quality of this approximation, and gives a guideline as to whether the line fit is plausible or not. The following tables are just the first 5 (200km to 400km) altitudes from the year 2000. It includes the data for all 19 of the sampling angel used to create the average for these altitudes. This is roughly 1/8<sup>th</sup> the total data for just the year 2000. The total data would be from 200km to 1950km.

	90						-10						
	size>=10	size>=10	size>=1m	size>=1cr	size>=10	size>=1m	size>=10	size>=10	size>=1m	size>=1cr	size>=10	size>=1m	
200	5.45E-02	9.82E-06	1.62E-08	1.53E-10	1.53E-10	1.53E-10	200	1.62E+00	3.91E-02	8.33E-05	1.19E-09	3.70E-10	2.45E-10
250	2.68E-02	2.17E-07	5.48E-09	1.24E-10	6.29E-11	6.29E-11	250	2.67E+00	7.07E-02	9.30E-05	1.49E-09	2.98E-10	1.55E-10
300	1.72E-01	2.93E-02	3.30E-06	3.72E-10	5.58E-11	5.39E-11	300	3.41E+00	1.19E-01	1.81E-04	3.54E-09	3.35E-10	2.77E-10
350	1.30E-01	7.90E-04	8.05E-07	7.54E-10	8.43E-11	5.50E-11	350	3.87E+00	1.46E-01	2.60E-04	6.61E-09	7.72E-10	3.59E-10
400	1.29E-01	7.59E-03	2.03E-06	5.39E-10	4.93E-10	5.91E-11	400	4.74E+00	1.57E-01	3.16E-04	6.93E-09	1.12E-09	5.76E-10
	80						-20						
200	9.81E-02	1.65E-04	6.66E-08	4.05E-10	4.05E-10	3.39E-10	200	2.48E+00	6.37E-02	1.29E-04	1.63E-09	4.71E-10	3.02E-10
250	2.31E-01	3.52E-02	2.10E-06	3.30E-10	3.30E-10	1.19E-10	250	4.12E+00	1.22E-01	1.79E-04	2.21E-09	4.02E-10	2.18E-10
300	2.02E-01	1.37E-02	7.09E-06	1.88E-09	5.85E-10	4.58E-10	300	5.03E+00	1.92E-01	3.09E-04	5.57E-09	3.99E-10	3.46E-10
350	3.41E-01	3.61E-03	8.01E-06	8.67E-09	1.34E-09	4.57E-10	350	5.59E+00	2.35E-01	3.99E-04	9.38E-09	9.27E-10	4.44E-10
400	3.48E-01	7.47E-03	1.27E-05	1.26E-08	3.18E-09	1.17E-09	400	6.81E+00	2.66E-01	4.84E-04	9.07E-09	1.32E-09	7.25E-10
	70						-30						
200	5.38E-02	4.57E-04	1.40E-07	3.02E-10	3.02E-10	3.02E-10	200	2.61E-01	3.79E-03	2.93E-05	2.61E-09	5.49E-10	2.97E-10
250	1.67E-01	1.26E-02	1.19E-06	2.03E-10	2.03E-10	8.44E-11	250	4.51E-01	1.40E-02	1.56E-05	2.00E-09	3.02E-10	1.46E-10
300	1.54E-01	4.82E-03	3.20E-06	1.49E-09	3.47E-10	2.11E-10	300	6.21E-01	1.19E-02	2.46E-05	2.35E-09	3.95E-10	3.26E-10
350	1.83E-01	4.26E-03	6.81E-06	6.86E-09	6.76E-10	2.55E-10	350	6.93E-01	2.79E-02	7.20E-05	5.19E-09	8.89E-10	4.11E-10
400	2.11E-01	3.81E-03	8.26E-06	1.08E-08	1.77E-09	6.70E-10	400	1.12E+00	3.15E-02	9.84E-05	6.26E-09	1.26E-09	6.49E-10
	60						-40						
200	4.21E-02	6.85E-04	1.42E-06	2.07E-10	2.07E-10	2.06E-10	200	3.13E-02	4.14E-04	8.54E-07	3.60E-10	3.60E-10	3.60E-10
250	1.26E-01	7.76E-03	1.36E-06	2.20E-10	2.20E-10	9.70E-11	250	8.15E-02	8.37E-03	2.32E-06	2.93E-10	2.90E-10	1.31E-10
300	1.34E-01	7.72E-03	8.61E-06	1.97E-09	2.74E-10	1.81E-10	300	1.02E-01	5.22E-03	7.54E-06	1.28E-09	3.52E-10	2.48E-10
350	1.78E-01	8.62E-03	1.36E-05	5.88E-09	6.48E-10	2.55E-10	350	1.14E-01	4.98E-03	1.16E-05	4.73E-09	1.02E-09	4.52E-10
400	1.67E-01	7.11E-03	1.53E-05	8.54E-09	1.65E-09	6.59E-10	400	1.28E-01	1.99E-03	8.60E-06	6.43E-09	1.45E-09	7.49E-10
	50						-50						
200	3.61E-02	3.68E-04	5.02E-07	3.31E-10	3.31E-10	3.31E-10	200	4.61E-02	6.54E-04	8.56E-07	3.52E-10	3.52E-10	3.52E-10
250	9.15E-02	1.19E-02	1.27E-06	2.86E-10	2.86E-10	9.66E-11	250	1.06E-01	1.56E-02	2.14E-06	3.01E-10	3.01E-10	1.01E-10
300	9.64E-02	3.55E-03	4.44E-06	1.30E-09	4.58E-10	3.04E-10	300	1.20E-01	4.37E-03	6.34E-06	1.55E-09	4.83E-10	3.41E-10
350	1.60E-01	6.14E-03	1.55E-05	5.47E-09	1.35E-09	6.05E-10	350	1.51E-01	7.03E-03	1.18E-05	6.06E-09	1.45E-09	6.64E-10
400	1.74E-01	3.37E-03	1.36E-05	7.40E-09	1.30E-09	5.44E-10	400	1.60E-01	3.36E-03	1.62E-05	7.87E-09	1.46E-09	6.25E-10
	40						-60						
200	6.26E-02	8.34E-04	4.45E-07	2.59E-10	2.59E-10	2.59E-10	200	4.58E-02	5.61E-04	5.49E-07	3.92E-10	3.92E-10	3.88E-10
250	1.20E-01	7.65E-03	3.12E-06	2.52E-10	2.52E-10	1.05E-10	250	1.76E-01	1.55E-02	3.12E-06	3.64E-10	3.64E-10	1.83E-10
300	2.54E-01	1.47E-02	2.68E-05	1.16E-09	3.12E-10	2.13E-10	300	2.13E-01	8.15E-03	1.04E-05	2.85E-09	3.52E-10	2.70E-10
350	3.65E-01	2.25E-02	6.01E-05	4.30E-09	8.67E-10	3.84E-10	350	2.27E-01	1.11E-02	3.12E-05	7.79E-09	8.08E-10	2.90E-10
400	5.06E-01	2.43E-02	7.82E-05	5.81E-09	1.23E-09	5.98E-10	400	3.09E-01	9.02E-03	4.80E-05	1.18E-08	2.08E-09	9.53E-10
	30						-70						
200	1.45E+00	3.52E-02	1.01E-04	2.16E-09	5.46E-10	3.06E-10	200	0.00E+00	0.00E+00	0.00E+00	0.00E+00	0.00E+00	0.00E+00
250	2.28E+00	5.79E-02	1.01E-04	2.82E-09	3.68E-10	2.05E-10	250	0.00E+00	0.00E+00	0.00E+00	0.00E+00	0.00E+00	0.00E+00
300	2.87E+00	7.95E-02	2.00E-04	6.14E-09	4.19E-10	3.20E-10	300	0.00E+00	0.00E+00	0.00E+00	0.00E+00	0.00E+00	0.00E+00
350	3.07E+00	1.06E-01	2.54E-04	1.01E-08	8.96E-10	4.16E-10	350	0.00E+00	0.00E+00	0.00E+00	0.00E+00	0.00E+00	0.00E+00
400	3.75E+00	1.06E-01	3.04E-04	9.58E-09	1.30E-09	6.50E-10	400	0.00E+00	0.00E+00	0.00E+00	0.00E+00	0.00E+00	0.00E+00
	20						-80						
200	2.03E+00	4.95E-02	1.03E-04	1.34E-09	4.02E-10	2.77E-10	200	1.66E-01	1.06E-03	2.58E-07	4.46E-10	4.46E-10	4.30E-10
250	3.42E+00	8.87E-02	1.24E-04	1.66E-09	3.22E-10	1.76E-10	250	3.62E-01	5.52E-02	3.92E-06	4.33E-10	4.33E-10	2.05E-10
300	4.28E+00	1.45E-01	2.14E-04	3.96E-09	3.79E-10	3.00E-10	300	3.61E-01	1.41E-02	6.39E-06	2.34E-09	8.89E-10	7.32E-10
350	4.90E+00	1.78E-01	2.94E-04	7.22E-09	8.10E-10	3.94E-10	350	5.41E-01	7.70E-03	9.88E-06	9.05E-09	1.92E-09	6.13E-10
400	6.10E+00	2.45E-01	4.20E-04	7.49E-09	1.19E-09	6.30E-10	400	5.86E-01	1.35E-02	1.54E-05	1.41E-08	4.34E-09	1.53E-09
	10						-90						
200	1.35E+00	3.65E-02	7.90E-05	1.13E-09	4.26E-10	3.05E-10	200	1.00E-05	1.27E-10	1.27E-10	1.27E-10	1.27E-10	0.00E+00
250	2.35E+00	7.52E-02	9.23E-05	1.37E-09	3.77E-10	1.99E-10	250	2.11E-07	1.94E-10	8.94E-11	8.94E-11	8.94E-11	0.00E+00
300	2.98E+00	9.52E-02	1.63E-04	3.25E-09	3.82E-10	3.13E-10	300	3.03E-02	2.91E-10	1.78E-10	1.09E-10	4.53E-11	0.00E+00
350	3.50E+00	1.33E-01	2.24E-04	6.30E-09	8.21E-10	4.05E-10	350	7.51E-04	4.69E-10	2.71E-10	1.44E-10	7.31E-11	0.00E+00
400	4.08E+00	1.35E-01	2.98E-04	6.72E-09	1.16E-09	6.09E-10	400	8.59E-03	4.84E-10	4.84E-10	4.84E-10	6.49E-11	0.00E+00
	0												
200	1.37E+00	3.57E-02	7.85E-05	1.10E-09	4.27E-10	3.16E-10							
250	2.16E+00	6.20E-02	8.77E-05	1.36E-09	3.71E-10	2.05E-10							
300	2.82E+00	9.61E-02	1.64E-04	3.23E-09	3.90E-10	3.37E-10							
350	3.26E+00	1.19E-01	2.37E-04	6.90E-09	8.43E-10	4.17E-10							
400	3.91E+00	1.48E-01	3.04E-04	6.71E-09	1.17E-09	6.25E-10							

Table 2 Data from the year 2000 including all 19 latitudes from 200 to 400km.

This information is then averaged together with the equations above to form the following table. This table contains the density average and standard deviation for a given altitude for each of my 6 size groupings.

	year = 2000											
	size>=10um	dev	size>=100um	dev	size>=1mm	dev	size>=1cm	dev	size>=10cm	dev	size>=1m	dev
200	5.94E-01	1.83E-01	1.42E-02	4.72E-03	3.20E-05	9.85E-06	1.51E-10	1.51E-10	3.56E-10	3.06E-11	2.82E-10	2.61E-11
250	1.01E+00	3.01E-01	3.60E-02	8.12E-03	3.76E-05	1.23E-05	8.43E-10	1.63E-10	2.89E-10	2.65E-11	1.35E-10	1.47E-11
300	1.27E+00	3.76E-01	4.47E-02	1.32E-02	7.07E-05	2.14E-05	2.41E-09	3.21E-10	3.83E-10	4.50E-11	2.92E-10	3.74E-11
350	1.45E+00	4.25E-01	5.48E-02	1.67E-02	1.01E-04	2.85E-05	6.22E-09	6.29E-10	9.00E-10	1.08E-10	3.79E-10	4.29E-11
400	1.76E+00	5.18E-01	6.18E-02	1.98E-02	1.29E-04	3.66E-05	7.84E-09	8.75E-10	1.56E-09	2.25E-10	6.77E-10	8.31E-11

**Table 3** The averaged data from table 2. This table Includes the standard deviation of the average.

At this point I need to break the six groupings apart and arrange them into their own tables spanning the nine years from 2000 to 2008. The following table is for all the averaged debris densities for the 10um size range. The graph contains the density for each latitude as well as the standard deviation for that density directly under it.

	2000	2001	2002	2003	10um 2004	2005	2006	2007	2008
200	0.59	0.62	0.52	0.56	0.69	0.78	1.20	1.10	1.05
error	0.18	0.19	0.16	0.17	0.22	0.25	0.39	0.35	0.44
250	1.01	1.00	0.91	0.87	1.07	1.22	1.66	1.43	1.46
error	0.30	0.29	0.26	0.25	0.32	0.37	0.51	0.44	0.51
300	1.27	1.37	1.35	1.26	1.42	1.48	1.97	1.77	1.74
error	0.37	0.41	0.40	0.37	0.42	0.44	0.59	0.52	0.57
350	1.45	1.65	1.54	1.57	1.69	1.82	2.35	2.23	2.09
error	0.42	0.48	0.45	0.46	0.50	0.52	0.65	0.60	0.68
400	1.76	1.86	1.77	1.90	1.99	2.29	2.90	2.82	2.62
error	0.51	0.54	0.52	0.55	0.58	0.63	0.76	0.72	0.81
450	2.26	2.35	2.25	2.45	2.55	2.96	4.01	4.01	3.76
error	0.62	0.65	0.62	0.68	0.69	0.73	0.88	0.85	0.90
500	2.43	2.52	2.34	2.51	2.67	3.06	4.10	4.16	3.97
error	0.72	0.74	0.69	0.75	0.76	0.81	0.96	0.96	0.96
550	2.81	2.80	2.64	2.85	3.10	3.60	4.86	4.90	4.88
error	0.81	0.81	0.77	0.84	0.86	0.90	1.03	1.01	1.06
600	3.20	3.15	2.98	3.22	3.53	4.22	5.44	5.86	5.93
error	0.85	0.87	0.82	0.91	0.92	0.98	1.12	1.12	1.18
650	3.77	3.60	3.44	3.70	4.13	4.99	6.20	6.82	7.05
error	0.93	0.95	0.89	1.01	1.01	1.11	1.23	1.24	1.27
700	4.41	4.15	3.97	4.25	4.84	5.77	7.12	7.73	8.16
error	0.96	0.98	0.93	1.05	1.07	1.18	1.32	1.30	1.39
750	5.01	4.73	4.43	4.77	5.49	6.51	7.83	8.54	8.81
error	1.03	1.05	0.98	1.12	1.15	1.26	1.41	1.41	1.57
800	5.48	5.32	4.99	5.28	5.86	7.04	8.34	9.24	9.34
error	1.12	1.13	1.07	1.21	1.25	1.39	1.54	1.60	1.71
850	6.16	6.06	5.63	5.88	6.38	7.52	8.74	9.72	9.78
error	1.22	1.23	1.15	1.30	1.34	1.49	1.66	1.75	1.77
900	6.86	6.66	6.31	6.55	7.07	8.02	9.20	10.22	10.17
error	1.28	1.28	1.21	1.36	1.41	1.55	1.72	1.83	1.89
950	7.76	7.60	7.06	7.32	8.04	8.91	9.93	10.99	11.01
error	1.39	1.39	1.30	1.44	1.51	1.66	1.82	1.95	1.93
1000	8.32	8.35	7.77	7.98	8.74	9.50	10.34	11.41	11.27
error	1.44	1.46	1.37	1.49	1.58	1.71	1.87	2.02	2.05
1050	9.20	9.23	8.61	8.74	9.66	10.42	11.15	12.28	12.04
error	1.56	1.57	1.48	1.57	1.69	1.83	1.99	2.15	2.16
1100	10.30	10.42	9.51	9.76	10.81	11.11	11.88	13.36	12.98
error	1.71	1.73	1.59	1.67	1.82	1.90	2.06	2.27	2.27
1150	11.37	11.69	10.56	10.91	11.67	11.71	12.81	14.18	13.56
error	1.88	1.93	1.75	1.83	1.96	2.00	2.20	2.40	2.28
1200	11.98	12.52	10.94	11.79	12.01	11.87	13.45	14.41	13.60
error	1.97	2.06	1.81	1.96	2.01	2.03	2.28	2.44	2.31
1250	12.38	12.76	10.93	12.06	11.78	11.83	13.64	14.20	13.61
error	2.06	2.12	1.83	2.01	2.00	2.05	2.33	2.46	2.27
1300	12.27	12.21	10.56	11.76	10.97	11.43	13.19	13.41	13.37
error	2.02	2.01	1.77	1.96	1.90	2.00	2.26	2.37	2.29
1350	12.36	11.69	10.26	11.35	10.47	11.20	12.74	12.88	13.40
error	2.05	1.94	1.74	1.91	1.87	1.98	2.20	2.34	2.33
1400	12.37	11.17	10.06	10.81	10.10	11.01	12.42	12.58	13.58
error	2.05	1.87	1.73	1.86	1.87	1.99	2.18	2.35	2.40
1450	12.55	10.79	10.12	10.23	9.86	11.02	12.14	12.73	14.18
error	2.08	1.83	1.74	1.80	1.86	1.98	2.14	2.34	2.21
1500	10.49	9.10	8.60	8.36	8.66	9.39	10.33	11.50	12.44
error	1.79	1.65	1.59	1.67	1.79	1.86	1.99	2.25	2.15
1550	9.04	7.92	7.59	7.25	7.91	8.38	9.13	10.54	11.12
error	1.67	1.60	1.57	1.69	1.80	1.86	1.97	2.25	2.12
1600	8.10	7.19	7.01	6.64	7.43	7.82	8.36	9.91	10.28
error	1.63	1.59	1.58	1.71	1.82	1.87	1.96	2.22	2.13
1650	7.21	6.59	6.33	6.24	6.92	7.32	7.76	9.28	9.37
error	1.63	1.60	1.61	1.75	1.85	1.91	1.99	2.24	2.10
1700	6.43	6.00	5.71	5.88	6.46	6.90	7.31	8.66	8.59
error	1.61	1.58	1.60	1.73	1.82	1.89	1.97	2.20	2.14
1750	5.90	5.74	5.49	5.83	6.31	6.72	7.13	8.41	8.21
error	1.64	1.62	1.63	1.76	1.85	1.93	2.01	2.24	2.15
1800	5.53	5.51	5.37	5.70	6.14	6.54	6.93	8.09	7.84
error	1.66	1.64	1.64	1.76	1.85	1.93	2.02	2.25	2.17
1850	5.34	5.32	5.28	5.56	6.02	6.36	6.79	7.79	7.53
error	1.66	1.66	1.65	1.76	1.86	1.93	2.05	2.26	2.24
1900	5.23	5.28	5.27	5.53	5.97	6.29	6.69	7.57	7.33
error	1.69	1.70	1.69	1.80	1.90	1.98	2.10	2.31	2.23
1950	5.11	5.20	5.17	5.44	5.86	6.16	6.57	7.33	7.12
error	1.68	1.70	1.68	1.79	1.90	1.97	2.10	2.29	0.00

Table 4 The averaged data for 10um from 200 to 1950km. The 3 highlighted regions are graphed in figures 6, 7 and 8.



These numbers now get inputted into the least square fit equations in order to make my predictions. I isolated three out of the 36 altitudes to look at more in depth. They cover three places of interest in the LEO region. 400km is where a few low-orbiting satellites can be found. It is also where the equatorial debris are much more dominant than the polar debris. 800km is near higher regions of orbit, and at this point the polar debris are more dominant. 800km also tends to be a greatly populated region of space for LEO satellites. 1200km would be rather high for a LEO satellite but it's still a populated region.

In order to fit a line to the graph I will be using the technique known as vertical least squares fitting <sup>7</sup>

$$R^2 = \sum [y_i - F(x_i, a_1, a_2, \dots, a_n)]^2$$

$$R^2(m, b) = \sum [y_i - (b + mx_i)]^2$$

$$\frac{d(R^2)}{dm} = -2 \sum [y_i - (b + mx_i)] x_i = 0$$

$$\frac{d(R^2)}{db} = -2 \sum [y_i - (b + mx_i)] = 0$$

After solving for b and m we get

$$b = \frac{\sum y \sum x^2 - \sum x \sum xy}{n \sum x^2 - (\sum x)^2} \quad m = \frac{n \sum xy - \sum x \sum y}{n \sum x^2 - (\sum x)^2}$$

These equations will create a line that best follows the data. The slope of the line is the current rate of increase in objects per cubic meter each year. By using this slope and intercept I was able to extend the line out to the year 2030. This is how I will be making my rough estimations for how much the debris around the earth might increase over 20 years.

---

<sup>7</sup> <http://mathworld.wolfram.com/LeastSquaresFitting.html>

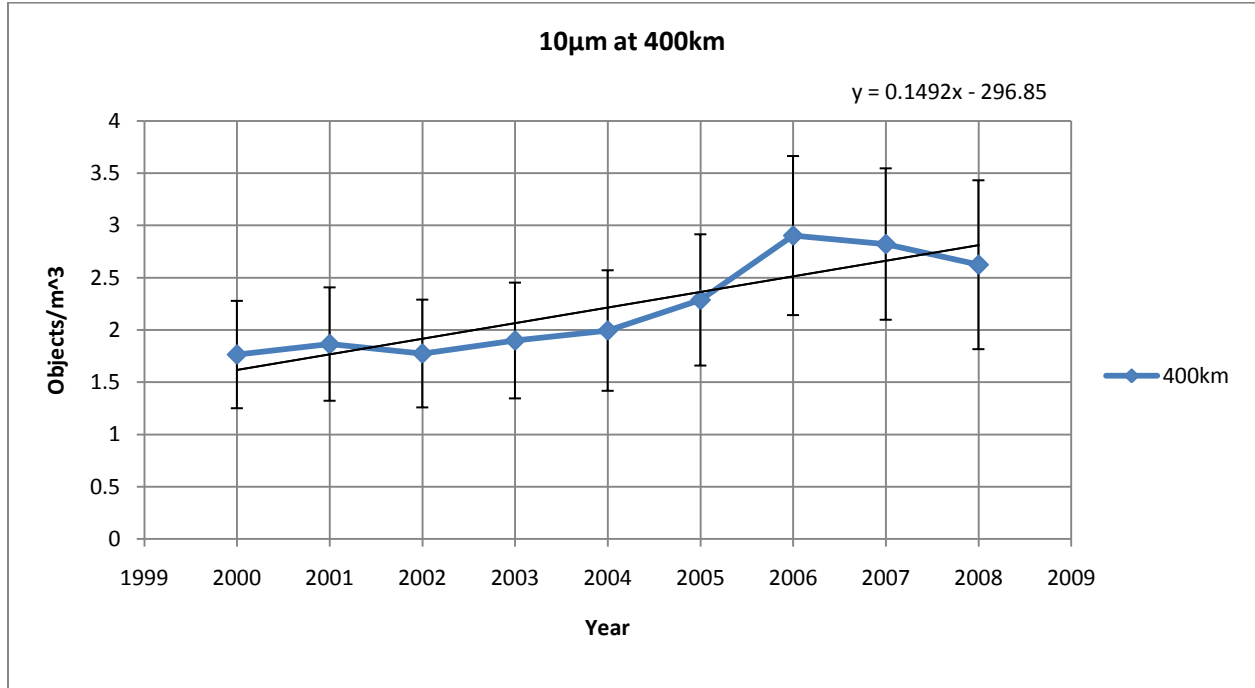


Figure 6 The 10µm objects/m<sup>3</sup> from 2000 to 2008 at 400km. This is the data from table 4. The error bars show the standard deviation.

According to the UCS satellite database there are only 13 satellites currently orbiting in this region and below.<sup>8</sup> Most of the debris is from satellite launches and tends to be clustered in the equatorial region which is why FIGURE 1 showed little activity outside the equator. Most of the debris in this region is unrelated to the satellites that occupy it. This is a region of great interest however, because the International Space Station orbits at around 400km.<sup>9</sup> Debris in this region will only stay there for several months or a few years.<sup>10</sup> This is why the region has such dramatically lower amounts of debris than the other two.

<sup>8</sup> UCS satellite database

<sup>9</sup> <http://spaceflight.nasa.gov/realdata/tracking/index.html>

<sup>10</sup> <http://www.orbitaldebris.jsc.nasa.gov/faqs.html#12>

Despite this rapid decay in debris, the debris in the region is still increasing quite rapidly. This means that the amount of debris entering the area is even larger than the data suggests, because it naturally has a faster decay rate.

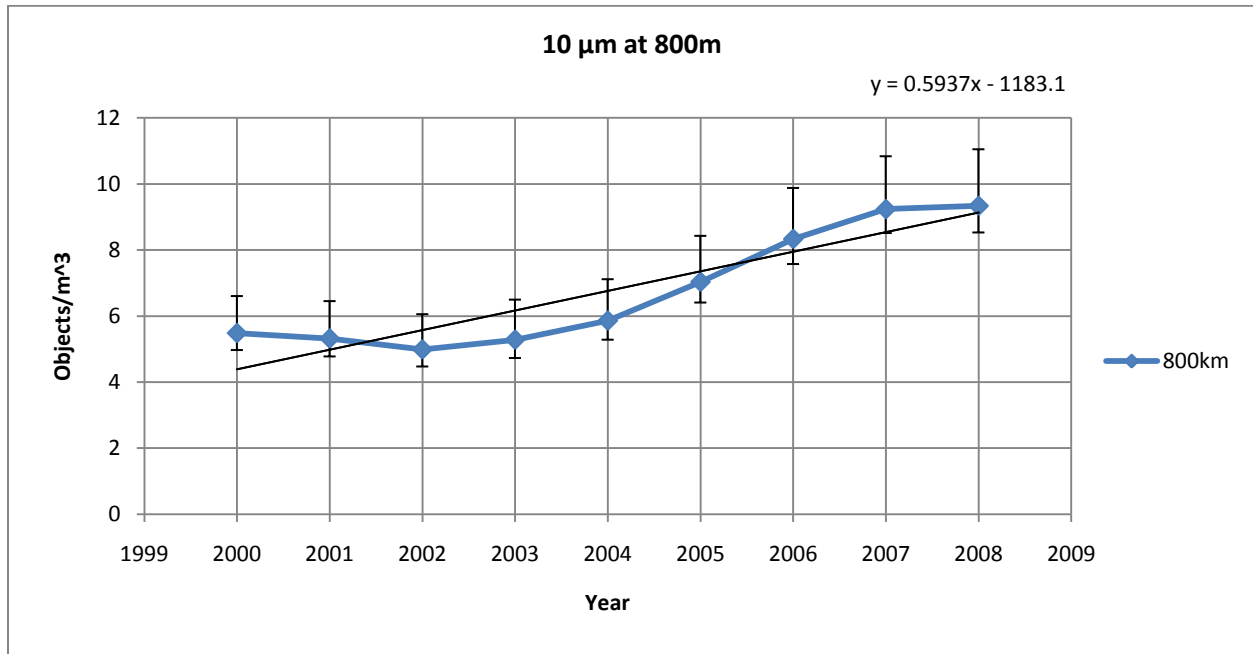


Figure 7 The 10μm objects/m³ from 2000 to 2008 at 800km. This is the data from table 4. The error bars show the standard deviation.

The vast majority of LEO satellites can be found in the region of space between the 800km and 1200km ranges. At around 800km, the time for orbital decay of space debris is measured in decades.<sup>11</sup> The high density of satellites and long persistence of space debris makes this region of space the largest danger zone for what is known as the Kessler syndrome<sup>12</sup>. Proposed by Donald J. Kessler, the Kessler syndrome describes how collisions between satellites and space debris could release more debris that would significantly elevate the risk of a collision. The implication is that the increased debris levels would lead to more collisions until the effect is so great that space exploration or satellites become unusable.

<sup>11</sup> <http://www.orbitaldebris.jsc.nasa.gov/faqs.html#12>

<sup>12</sup> *Collisional cascading: The limits of population growth in low earth orbit*

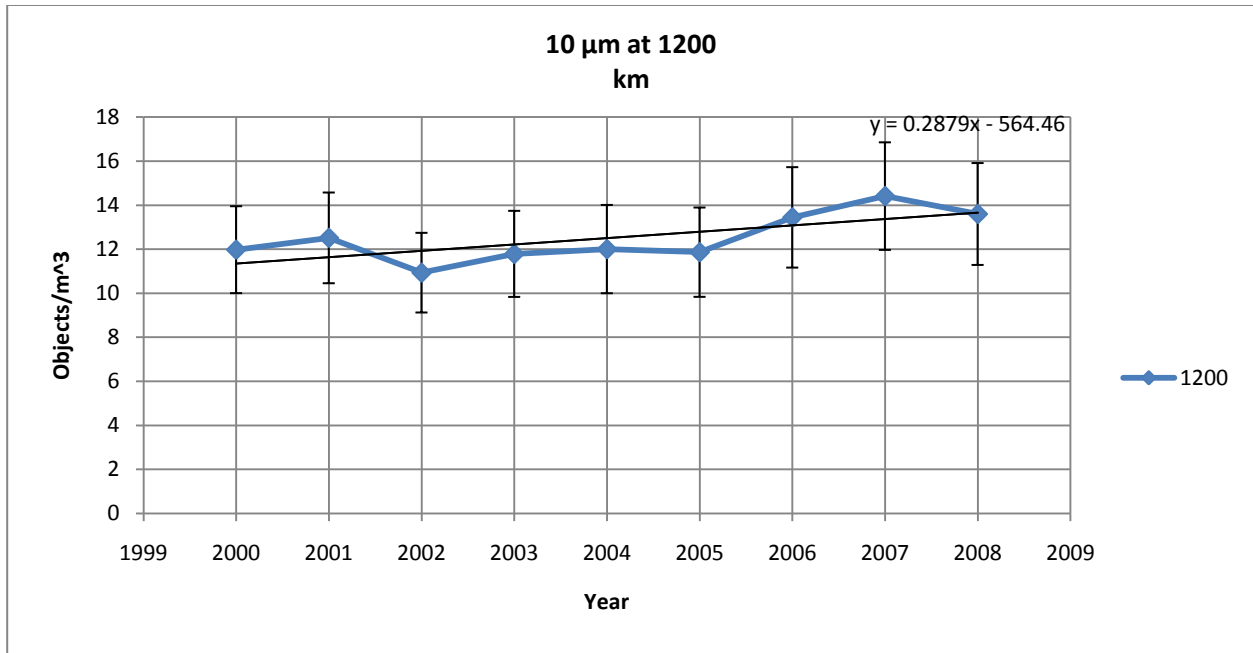


Figure 8 The 10μm objects/m<sup>3</sup> from 2000 to 2008 at 1200km. This is the data from table 4. The error bars show the standard deviation.

The peak of debris is around the 1200km mark. Past 1000km, the debris orbital lifetime is no longer measured in decades, but instead in centuries.<sup>13</sup> Everything we put into space at this altitude is going to stay there for a very significant amount of them. Some satellites are able to force themselves into a decaying orbit near the end of their missions, but many are unable to do so due to mechanical or power failure.

The goodness of fit calculation is a measurement of how well the line fit is approximating the data. . R<sup>2</sup> off .9 and .8 are decent approximations, .6 and .7 are so-so, and anything .5 or less is a poor approximation. The equation for R<sup>2</sup> in vector form is<sup>14</sup>

$$\frac{(\sum(xi - \bar{x})(yi - \bar{y}))^2}{\sum(xi - \bar{x})^2 \sum(yi - \bar{y})^2} = r^2$$

<sup>13</sup> <http://www.orbitaldebris.jsc.nasa.gov/faqs.html#12>

<sup>14</sup> <http://mathworld.wolfram.com/LeastSquaresFitting.html>

This was enough information in make my predictions for the increase in the debris levels in the LEO. The following six tables are the final results for this calculation. They contain the data from the year 2000 to 2030 every 5 years, as well as the percent increase from the year 2000 to the year 2030. The r<sup>2</sup> value shows how well I am able to fit a line to the data.

	Year	10um							2000 -> 2030	R <sup>2</sup>
		2000	2005	2010	2015	2020	2025	2030		
		altitude in km	200	0.59354	0.78449	1.27586	1.67979	2.08371		
	250	1.00831	1.22475	1.67787	2.0911	2.50433	2.91756	3.33079	230.34%	0.66508
	300	1.26746	1.47653	1.9678	2.34544	2.72308	3.10071	3.47835	174.44%	0.67939
	350	1.44825	1.81738	2.44351	2.96161	3.47971	3.9978	4.5159	211.82%	0.75262
	400	1.7645	2.28718	3.11012	3.85628	4.60244	5.3486	6.09476	245.41%	0.79433
	450	2.25904	2.95779	4.45582	5.70631	6.95679	8.20728	9.45777	318.66%	0.80976
	500	2.43365	3.05979	4.60162	5.86446	7.1273	8.39014	9.65299	296.65%	0.8003
	550	2.81317	3.59816	5.58163	7.22881	8.87599	10.5232	12.1704	332.62%	0.82249
	600	3.2036	4.21924	6.66256	8.73952	10.8165	12.8935	14.9704	367.30%	0.84598
	650	3.77223	4.991	7.8112	10.2747	12.7382	15.2017	17.6652	368.30%	0.85188
	700	4.40571	5.77026	8.95781	11.7574	14.557	17.3566	20.1562	357.50%	0.8533
	750	5.01083	6.5103	9.75482	12.6864	15.6181	18.5497	21.4813	328.70%	0.84854
	800	5.48413	7.03645	10.3273	13.2959	16.2645	19.2331	22.2017	304.83%	0.83984
	850	6.15966	7.51705	10.6466	13.4197	16.1929	18.966	21.7391	252.93%	0.81845
	900	6.85705	8.02104	11.0114	13.6083	16.2052	18.8021	21.399	212.07%	0.81463
	950	7.76321	8.91409	11.7863	14.3274	16.8685	19.4096	21.9507	182.75%	0.80494
	1000	8.32071	9.49655	12.0627	14.3684	16.6741	18.9799	21.2856	155.81%	0.80975
	1050	9.20379	10.4238	12.8749	15.1472	17.4195	19.6918	21.9641	138.64%	0.79806
	1100	10.3004	11.1142	13.6913	15.8291	17.967	20.1049	22.2428	115.94%	0.74198
	1150	11.3677	11.7071	14.2022	15.9949	17.7877	19.5804	21.3732	88.02%	0.65612
	1200	11.9787	11.8652	14.2326	15.6721	17.1116	18.5511	19.9907	66.88%	0.51613
	1250	12.3829	11.8278	14.0174	15.2174	16.4173	17.6173	18.8173	51.96%	0.38124
	1300	12.27	11.4347	13.4267	14.5061	15.5856	16.665	17.7444	44.62%	0.319
	1350	12.3616	11.1958	13.0735	14.1193	15.1651	16.2109	17.2567	39.60%	0.27168
	1400	12.3743	11.0075	12.9618	14.1239	15.2859	16.4479	17.61	42.31%	0.2721
	1450	12.5465	11.0173	13.2307	14.6622	16.0937	17.5252	18.9568	51.09%	0.28689
	1500	10.4878	9.38773	11.8236	13.4483	15.0731	16.6978	18.3226	74.70%	0.39449
	1550	9.03692	8.38464	10.8048	12.5068	14.2088	15.9108	17.6127	94.90%	0.48966
	1600	8.09987	7.81648	10.1591	11.89	13.6209	15.3519	17.0828	110.90%	0.56196
	1650	7.21213	7.32025	9.51516	11.2374	12.9596	14.6818	16.404	127.45%	0.64947
	1700	6.42652	6.89764	8.96377	10.6998	12.4357	14.1717	15.9077	147.53%	0.73929
	1750	5.90122	6.72435	8.77657	10.5595	12.3424	14.1253	15.9082	169.57%	0.82332
	1800	5.53378	6.5441	8.49656	10.2379	11.9793	13.7207	15.4621	179.41%	0.86989
	1850	5.33852	6.36438	8.22063	9.8862	11.5518	13.2173	14.8829	178.78%	0.89231
	1900	5.22861	6.28768	8.01296	9.58401	11.1551	12.7261	14.2972	173.44%	0.91232
	1950	5.11244	6.15533	7.7865	9.27987	10.7732	12.2666	13.76	169.15%	0.92027

Table 5 The 10µm debris trend shortened into 5 year snapshots. This includes the percent increase in density from the year 2000 to the year 2030, as well as the goodness of fit value for the measurement of how well the data fit a linear approximation.

In the 10 $\mu$ m graph, the first thing I notice is that I have really poor values for R<sup>2</sup> around the 1400 mark. In this region of space the amount of debris currently entering area is very low. We see a correlation between the percentage of increase and the value for r<sup>2</sup>. However, when I looked at the highest percent increase, I saw a diminished value for r<sup>2</sup> again. The 200km data show an alarmingly high increase, but only manages to get an r<sup>2</sup> value of .73. This is because exponential or power series might fit that particular data better.

The 600-800 km region shows a large and consistently liner growth of debris. The entire region is expected to get a 300% increase in this 30-year span. This is the important area to watch because of its high population of satellites, debris, and long decay periods.

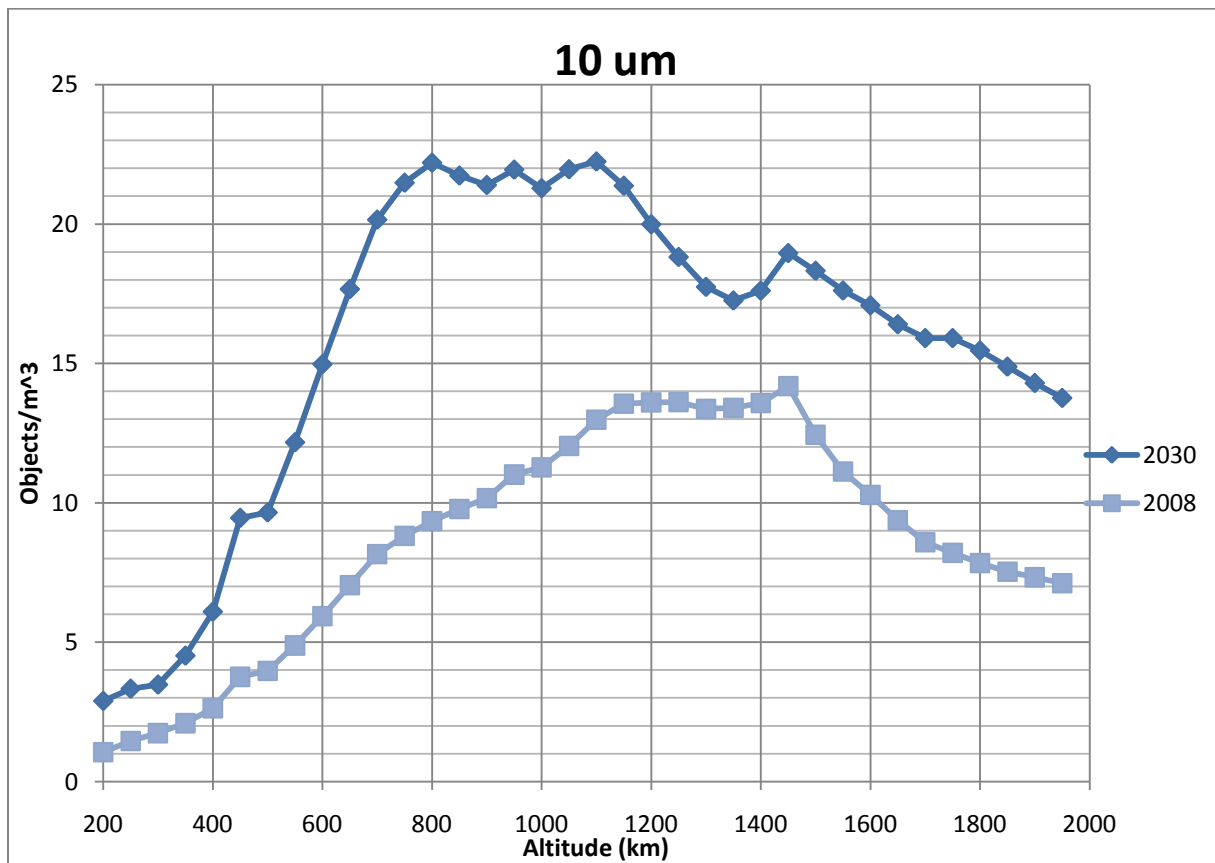


Figure 9 The 10 $\mu$ m objects/m<sup>3</sup> at 2008 and 2030 from 200km to 1950km.

		100um							2000 -> 2030	R^2
		Year								
		2000	2005	2010	2015	2020	2025	2030		
	200	0.01421	0.01671	0.02588	0.03299	0.04009	0.04719	0.05429	282.05%	0.74475
	250	0.03596	0.03243	0.04276	0.0477	0.05264	0.05758	0.06253	73.86%	0.41277
altitude	300	0.04472	0.04058	0.05509	0.06138	0.06768	0.07398	0.08028	79.53%	0.40929
in km	350	0.05483	0.05194	0.06963	0.07822	0.08681	0.0954	0.10399	89.65%	0.48753
	400	0.06179	0.06156	0.08173	0.09434	0.10696	0.11957	0.13219	113.94%	0.70715
	450	0.0757	0.07701	0.10275	0.12141	0.14007	0.15873	0.1774	134.35%	0.74171
	500	0.09429	0.10058	0.13793	0.16777	0.19762	0.22746	0.2573	172.89%	0.73459
	550	0.1196	0.13856	0.23198	0.30457	0.37716	0.44975	0.52234	336.74%	0.73976
	600	0.14453	0.16997	0.29494	0.392	0.48905	0.58611	0.68317	372.68%	0.74888
	650	0.18109	0.2305	0.44737	0.61574	0.7841	0.95247	1.12083	518.92%	0.7414
	700	0.20881	0.28873	0.53464	0.73696	0.93929	1.14161	1.34394	543.61%	0.79865
	750	0.25234	0.36635	0.59262	0.80352	1.01442	1.22532	1.43622	469.17%	0.81552
	800	0.27983	0.37472	0.61402	0.82672	1.03943	1.25213	1.46484	423.47%	0.79142
	850	0.3215	0.43703	0.76943	1.04984	1.33025	1.61066	1.89107	488.20%	0.83208
	900	0.33038	0.57351	0.98479	1.36258	1.74036	2.11815	2.49594	655.48%	0.92914
	950	0.29845	0.55686	0.90904	1.24628	1.58351	1.92075	2.25799	656.56%	0.96731
	1000	0.26804	0.53576	0.76129	1.01224	1.26318	1.51412	1.76506	558.51%	0.97996
	1050	0.33217	0.64353	0.88537	1.16361	1.44184	1.72007	1.99831	501.59%	0.98503
	1100	0.50495	0.92105	1.26075	1.63099	2.00124	2.37149	2.74174	442.97%	0.96702
	1150	0.6775	1.10217	1.44698	1.79858	2.15017	2.50176	2.85336	321.16%	0.91145
	1200	0.85289	1.25388	1.54888	1.82851	2.10814	2.38778	2.66741	212.75%	0.77389
	1250	1.00786	1.35658	1.53046	1.71507	1.89969	2.0843	2.26891	125.12%	0.59558
	1300	1.15276	1.38607	1.51176	1.63599	1.76022	1.88445	2.00868	74.25%	0.58443
	1350	1.38625	1.43562	1.55353	1.62864	1.70374	1.77885	1.85395	33.74%	0.25893
	1400	1.60557	1.49614	1.62018	1.67283	1.72547	1.77812	1.83077	14.03%	0.06861
	1450	1.66704	1.44214	1.61877	1.70662	1.79447	1.88232	1.97018	18.18%	0.10455
	1500	1.26201	1.04459	1.3005	1.42916	1.55782	1.68649	1.81515	43.83%	0.20644
	1550	0.75743	0.65159	0.81898	0.90584	0.9927	1.07956	1.16643	54.00%	0.20668
	1600	0.46148	0.42143	0.57414	0.65946	0.74477	0.83009	0.91541	98.36%	0.26146
	1650	0.27588	0.26501	0.3846	0.45014	0.51567	0.58121	0.64674	134.43%	0.4092
	1700	0.20364	0.2219	0.28633	0.33393	0.38152	0.42912	0.47671	134.09%	0.79998
	1750	0.18806	0.20734	0.25737	0.29764	0.33792	0.3782	0.41848	122.53%	0.91561
	1800	0.18771	0.21044	0.26036	0.30188	0.34339	0.3849	0.42641	127.17%	0.92946
	1850	0.18614	0.21152	0.26128	0.30364	0.34599	0.38835	0.43071	131.39%	0.94385
	1900	0.18204	0.2118	0.26004	0.30281	0.34558	0.38836	0.43113	136.83%	0.96544
	1950	0.18425	0.21627	0.2654	0.30941	0.35343	0.39744	0.44145	139.59%	0.97003

Table 6 The 100µm debris trend shortened into 5 year snapshots. This includes the percent increase in density from the year 2000 to the year 2030, as well as the goodness of fit value for the measurement of how well the data fit a linear approximation.

In the 100um results I see an even larger increase in the 600km to 1100km region, peaking at around a 650% increase with a .96 value for r^2. I continued to see an increase in the

200km region, but much lower amounts of debris in the 250-400km region than the 10um results. An unexpected but continuing trend is the accurate increase in the debris near the 2000km region.

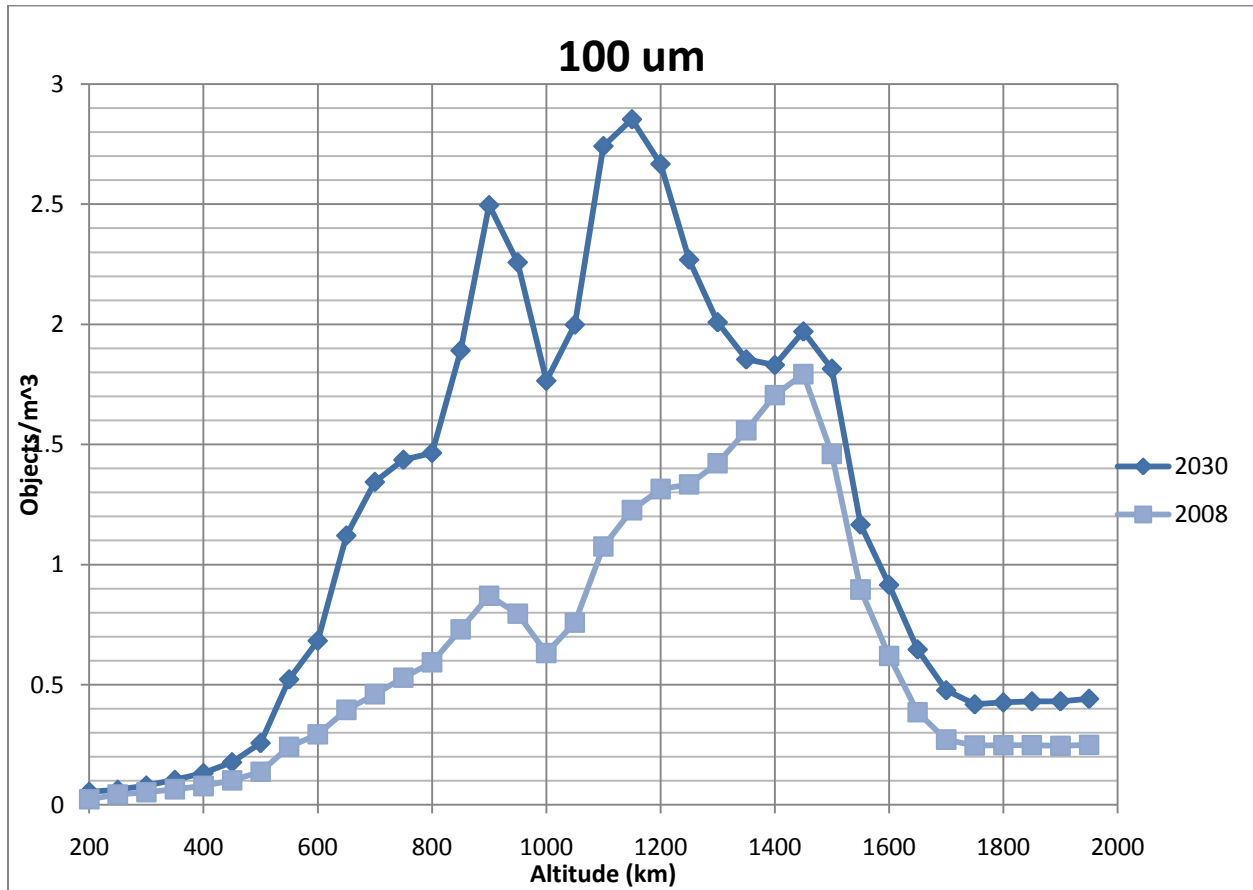


Figure 10 The 100µm objects/m<sup>3</sup> at 2008 and 2030 from 200km to 1950km.



		1mm							2000 -> 2030	R^2
		Year								
		2000	2005	2010	2015	2020	2025	2030		
	200	3.2E-05	3.9E-05	6.3E-05	8.1E-05	9.9E-05	0.00012	0.00013	319.24%	0.81161
	250	3.8E-05	3.8E-05	5.4E-05	6.5E-05	7.6E-05	8.6E-05	9.7E-05	156.87%	0.69061
altitude in km	300	7.1E-05	6.9E-05	9.5E-05	0.00011	0.00012	0.00014	0.00015	112.24%	0.6005
	350	0.0001	0.0001	0.00014	0.00016	0.00018	0.0002	0.00022	115.87%	0.62794
	400	0.00013	0.00013	0.00018	0.00021	0.00024	0.00027	0.0003	128.64%	0.78512
	450	0.0002	0.0002	0.00027	0.00032	0.00037	0.00042	0.00047	141.41%	0.79167
	500	0.00024	0.00025	0.00033	0.00039	0.00045	0.00051	0.00057	137.30%	0.76158
	550	0.00026	0.00029	0.00039	0.00047	0.00055	0.00063	0.00071	171.78%	0.76708
	600	0.0003	0.00034	0.00045	0.00055	0.00065	0.00075	0.00085	189.17%	0.79009
	650	0.00033	0.00039	0.00054	0.00066	0.00079	0.00091	0.00104	210.83%	0.80826
	700	0.00037	0.00043	0.00059	0.00073	0.00087	0.001	0.00114	211.76%	0.83923
	750	0.00044	0.00053	0.00068	0.00083	0.00099	0.00114	0.00129	195.87%	0.84866
	800	0.00029	0.00034	0.00044	0.00054	0.00063	0.00073	0.00082	187.32%	0.87406
	850	0.0002	0.00025	0.00032	0.00038	0.00045	0.00051	0.00057	186.73%	0.94277
	900	0.00022	0.00026	0.00034	0.00041	0.00048	0.00054	0.00061	175.73%	0.87434
	950	0.00039	0.00049	0.00065	0.0008	0.00095	0.0011	0.00125	222.61%	0.93258
	1000	0.00055	0.00075	0.00096	0.00117	0.00139	0.00161	0.00182	230.51%	0.97098
	1050	0.00048	0.00064	0.0008	0.00098	0.00115	0.00133	0.0015	209.99%	0.97772
	1100	0.00041	0.00053	0.00067	0.00081	0.00095	0.00109	0.00122	195.90%	0.97394
	1150	0.00035	0.00044	0.00055	0.00065	0.00075	0.00085	0.00094	168.02%	0.9638
	1200	0.00034	0.00042	0.00051	0.0006	0.00068	0.00077	0.00085	151.13%	0.96264
1250	0.0004	0.00047	0.00057	0.00065	0.00074	0.00082	0.00091	127.91%	0.97347	
1300	0.00045	0.00053	0.00062	0.00071	0.0008	0.00089	0.00098	118.71%	0.98794	
1350	0.0005	0.00056	0.00066	0.00074	0.00082	0.0009	0.00098	93.75%	0.94195	
1400	0.00056	0.00059	0.00068	0.00075	0.00081	0.00088	0.00095	69.04%	0.80704	
1450	0.00057	0.00055	0.00063	0.00068	0.00073	0.00078	0.00083	45.68%	0.55408	
1500	0.00051	0.00049	0.00057	0.00062	0.00067	0.00073	0.00078	53.49%	0.54256	
1550	0.00038	0.00039	0.00046	0.00051	0.00056	0.00062	0.00067	73.99%	0.69718	
1600	0.0003	0.00032	0.00039	0.00044	0.00049	0.00054	0.00059	95.00%	0.76395	
1650	0.00028	0.0003	0.00037	0.00043	0.00048	0.00053	0.00059	107.22%	0.82536	
1700	0.0003	0.00032	0.0004	0.00046	0.00052	0.00058	0.00064	114.17%	0.88472	
1750	0.00029	0.00032	0.00039	0.00045	0.00051	0.00057	0.00063	120.62%	0.91735	
1800	0.00025	0.00028	0.00035	0.0004	0.00046	0.00051	0.00057	126.88%	0.93005	
1850	0.00026	0.0003	0.00037	0.00043	0.00049	0.00055	0.00061	131.28%	0.94563	
1900	0.00026	0.0003	0.00037	0.00043	0.00049	0.00055	0.00061	136.75%	0.96481	
1950	0.00023	0.00028	0.00034	0.00039	0.00045	0.00051	0.00056	139.55%	0.97003	

Table 7 The 1mm debris trend shortened into 5 year snapshots. This includes the percent increase in density from the year 2000 to the year 2030, as well as the goodness of fit value for the measurement of how well the data fit a linear approximation.

The 1mm results are a more subdued version of the first two. There is a smaller but definite increase in the region around 800km. Another clear increase appears in the 200km space with a curious increase near the 2000km mark.

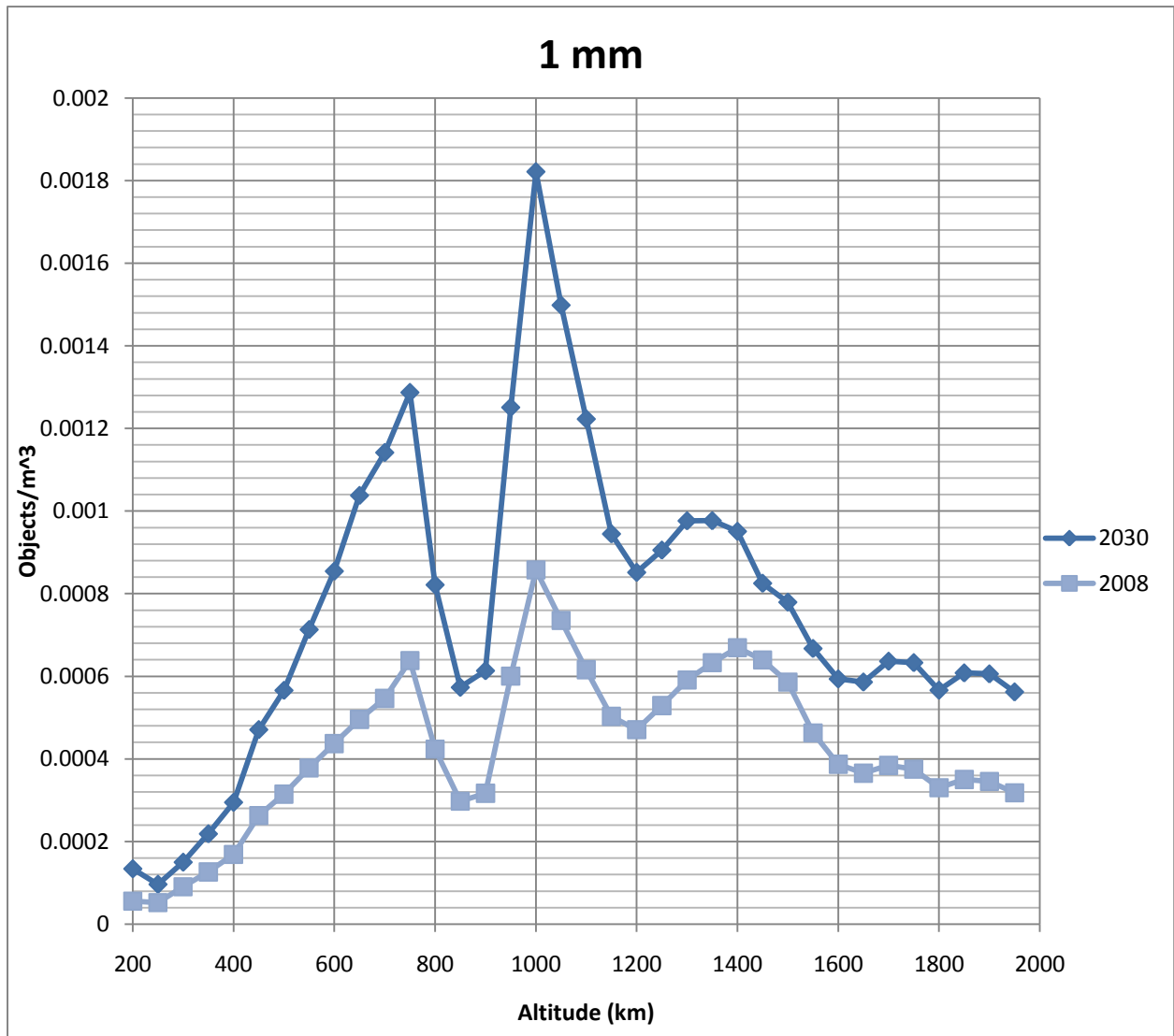


Figure 11 The 1mm objects/m<sup>3</sup> at 2008 and 2030 from 200km to 1950km.

		1cm								
		Year								
		2000	2005	2010	2015	2020	2025	2030	2000 -> 2030	R^2
altitude in km	200	7.8E-10	2.5E-09	5E-09	6.5E-09	8.1E-09	9.7E-09	1.1E-08	1359.21%	0.45558
	250	8.4E-10	1.3E-09	2E-09	2.5E-09	3E-09	3.4E-09	3.9E-09	359.63%	0.44676
	300	2.4E-09	4.2E-09	6.7E-09	8.7E-09	1.1E-08	1.3E-08	1.4E-08	499.48%	0.76435
	350	6.2E-09	9.9E-09	1.5E-08	1.9E-08	2.4E-08	2.8E-08	3.3E-08	429.50%	0.95102
	400	7.8E-09	1.4E-08	2.1E-08	2.7E-08	3.4E-08	4E-08	4.7E-08	495.06%	0.85676
	450	2.4E-08	3.5E-08	5.5E-08	7.3E-08	9E-08	1.1E-07	1.3E-07	420.42%	0.88305
	500	2.3E-08	3.2E-08	4.8E-08	6.1E-08	7.3E-08	8.6E-08	9.9E-08	323.05%	0.87362
	550	3.8E-08	3.8E-08	5.1E-08	6.1E-08	7.1E-08	8.1E-08	9.1E-08	140.64%	0.54148
	600	4.3E-08	5.1E-08	7.3E-08	9.1E-08	1.1E-07	1.3E-07	1.5E-07	240.05%	0.80159
	650	5.8E-08	6.8E-08	8.6E-08	1E-07	1.2E-07	1.4E-07	1.5E-07	164.81%	0.87917
	700	7.6E-08	8.8E-08	1.1E-07	1.3E-07	1.4E-07	1.6E-07	1.8E-07	137.69%	0.87599
	750	1.2E-07	1.4E-07	1.7E-07	2.1E-07	2.4E-07	2.7E-07	3E-07	146.03%	0.86724
	800	2.2E-07	2.7E-07	3.3E-07	3.9E-07	4.5E-07	5.1E-07	5.8E-07	166.16%	0.94794
	850	4.1E-07	5.8E-07	6.4E-07	7.3E-07	8.1E-07	8.9E-07	9.7E-07	136.54%	0.66641
	900	4.6E-07	3.4E-07	2.9E-07	2.3E-07	1.7E-07	1E-07	4E-08	-91.37%	0.69911
	950	2.6E-07	2.5E-07	2.7E-07	2.9E-07	3E-07	3.2E-07	3.3E-07	28.38%	0.33404
	1000	1.1E-07	1.2E-07	1.3E-07	1.4E-07	1.5E-07	1.6E-07	1.7E-07	47.67%	0.79864
	1050	7.9E-08	7.3E-08	7.2E-08	7E-08	6.9E-08	6.7E-08	6.5E-08	-17.89%	0.20921
	1100	6.3E-08	6.2E-08	6.6E-08	6.9E-08	7.2E-08	7.4E-08	7.7E-08	22.02%	0.36019
1150	5.2E-08	5.5E-08	6.3E-08	6.9E-08	7.5E-08	8.1E-08	8.7E-08	66.46%	0.76767	
1200	5.2E-08	6E-08	7.2E-08	8.2E-08	9.3E-08	1E-07	1.1E-07	116.73%	0.92011	
1250	7.8E-08	9.1E-08	1.1E-07	1.3E-07	1.4E-07	1.6E-07	1.8E-07	128.54%	0.91389	
1300	9.4E-08	1.2E-07	1.4E-07	1.7E-07	1.9E-07	2.1E-07	2.4E-07	152.44%	0.96551	
1350	9.6E-08	1.2E-07	1.4E-07	1.6E-07	1.8E-07	2E-07	2.2E-07	125.28%	0.97638	
1400	9.7E-08	1.1E-07	1.2E-07	1.4E-07	1.5E-07	1.7E-07	1.8E-07	83.60%	0.95891	
1450	8.7E-08	8.9E-08	9.3E-08	9.7E-08	1E-07	1E-07	1.1E-07	22.36%	0.80111	
1500	7.7E-08	7.6E-08	7.9E-08	8.1E-08	8.3E-08	8.4E-08	8.6E-08	11.63%	0.47432	
1550	4.9E-08	5.1E-08	5.5E-08	5.8E-08	6.1E-08	6.4E-08	6.7E-08	38.71%	0.88296	
1600	3.3E-08	3.5E-08	3.9E-08	4.2E-08	4.5E-08	4.7E-08	5E-08	52.99%	0.91971	
1650	3.1E-08	3.3E-08	3.6E-08	3.9E-08	4.2E-08	4.4E-08	4.7E-08	51.91%	0.93276	
1700	2.8E-08	2.9E-08	3.2E-08	3.4E-08	3.6E-08	3.8E-08	4E-08	42.91%	0.8319	
1750	2E-08	2.2E-08	2.5E-08	2.8E-08	3E-08	3.3E-08	3.5E-08	74.71%	0.90601	
1800	1.4E-08	1.6E-08	1.8E-08	2.1E-08	2.3E-08	2.5E-08	2.8E-08	97.65%	0.91721	
1850	1.5E-08	1.7E-08	2E-08	2.3E-08	2.5E-08	2.8E-08	3E-08	101.32%	0.95459	
1900	1.5E-08	1.7E-08	2E-08	2.2E-08	2.5E-08	2.7E-08	2.9E-08	95.54%	0.94666	
1950	1.2E-08	1.4E-08	1.7E-08	1.9E-08	2.2E-08	2.4E-08	2.6E-08	113.71%	0.95604	

Table 8 The 1cm debris trend shortened into 5 year snapshots. This includes the percent increase in density from the year 2000 to the year 2030, as well as the goodness of fit value for the measurement of how well the data fit a linear approximation.

The 200km data immediately jumped out at me. Over %1000 increase is much more substantial than anything I had seen thus far, However the r^2 number paints a different picture.

This region of space has very few objects this large. The data were far too inconsistent to predict anything in that area. The 200km to 400km region does show a dramatic increase which seems to be accurate. This growth is much larger than the 800km region which is another new trend.

This table also contained my first calculated decrease in space debris. The 1050 data appear to be extremely inconsistent; however the 900km seems to be fairly accurate. It looks like it is overestimating, but there is a clear fall off in density increase around the 900km mark. Once again there is a clear increase near the 2000km mark with a large value for  $r^2$  backing it up.

		10cm								
		Year								
		2000	2005	2010	2015	2020	2025	2030	2000 -> 2030	R^2
altitude in km	200	3.6E-10	2.7E-10	3.4E-10	3.5E-10	3.6E-10	3.7E-10	3.8E-10	7.41%	0.01683
	250	2.9E-10	1.8E-10	2.4E-10	2.5E-10	2.6E-10	2.7E-10	2.8E-10	-3.60%	0.0118
	300	3.8E-10	5.6E-10	7.4E-10	8.9E-10	1E-09	1.2E-09	1.3E-09	248.15%	0.52345
	350	9E-10	1E-09	1.4E-09	1.7E-09	2E-09	2.3E-09	2.6E-09	190.94%	0.75837
	400	1.6E-09	1.5E-09	1.9E-09	2.3E-09	2.6E-09	3E-09	3.3E-09	114.36%	0.50778
	450	2.7E-09	2.9E-09	4E-09	4.9E-09	5.8E-09	6.7E-09	7.6E-09	185.99%	0.66661
	500	5.1E-09	5E-09	6.2E-09	6.8E-09	7.5E-09	8.1E-09	8.8E-09	71.12%	0.5612
	550	6.9E-09	5.3E-09	6.1E-09	6.2E-09	6.4E-09	6.5E-09	6.7E-09	-2.98%	0.00885
	600	8.6E-09	8.2E-09	9.1E-09	9.5E-09	9.9E-09	1E-08	1.1E-08	23.79%	0.27503
	650	8.7E-09	7.3E-09	7.8E-09	7.8E-09	7.9E-09	8E-09	8.1E-09	-7.39%	0.004
	700	9.2E-09	9.9E-09	1.2E-08	1.4E-08	1.5E-08	1.7E-08	1.8E-08	100.33%	0.84874
	750	2E-08	1.8E-08	1.9E-08	2E-08	2.1E-08	2.2E-08	2.3E-08	16.37%	0.13452
	800	1.7E-08	1.6E-08	1.8E-08	1.9E-08	2E-08	2.1E-08	2.3E-08	35.97%	0.37135
	850	1.4E-08	1.4E-08	1.5E-08	1.5E-08	1.6E-08	1.7E-08	1.7E-08	23.54%	0.59127
	900	1.5E-08	1.6E-08	1.7E-08	1.8E-08	1.9E-08	2E-08	2.1E-08	35.32%	0.74649
	950	2.1E-08	2.3E-08	2.6E-08	2.9E-08	3.2E-08	3.5E-08	3.8E-08	77.13%	0.95245
	1000	1.3E-08	1.3E-08	1.4E-08	1.5E-08	1.6E-08	1.7E-08	1.8E-08	44.75%	0.86147
	1050	9.5E-09	9.3E-09	9.5E-09	9.6E-09	9.7E-09	9.8E-09	1E-08	4.32%	0.13905
	1100	6E-09	6E-09	6.2E-09	6.4E-09	6.5E-09	6.7E-09	6.8E-09	13.20%	0.4359
1150	4.4E-09	4.4E-09	4.7E-09	5E-09	5.2E-09	5.5E-09	5.7E-09	29.25%	0.61514	
1200	3E-09	3.2E-09	3.7E-09	4.1E-09	4.5E-09	4.9E-09	5.3E-09	75.40%	0.87987	
1250	4.9E-09	5.3E-09	6.5E-09	7.3E-09	8.2E-09	9.1E-09	1E-08	102.28%	0.86864	
1300	3.6E-09	3.9E-09	4.5E-09	4.9E-09	5.3E-09	5.7E-09	6.2E-09	69.71%	0.90687	
1350	5E-09	5.5E-09	6.3E-09	6.9E-09	7.6E-09	8.3E-09	9E-09	80.86%	0.99309	
1400	1.1E-08	1.2E-08	1.5E-08	1.7E-08	1.9E-08	2.2E-08	2.4E-08	123.07%	0.94953	
1450	1.2E-08	1.2E-08	1.3E-08	1.4E-08	1.4E-08	1.5E-08	1.5E-08	30.59%	0.90203	
1500	7.3E-09	7.2E-09	7.5E-09	7.6E-09	7.7E-09	7.9E-09	8E-09	10.49%	0.58239	
1550	3.2E-09	3.3E-09	3.5E-09	3.7E-09	3.9E-09	4.1E-09	4.2E-09	31.67%	0.85679	
1600	2.5E-09	2.5E-09	2.7E-09	2.9E-09	3E-09	3.1E-09	3.3E-09	32.76%	0.80942	
1650	2.4E-09	2.5E-09	2.7E-09	2.8E-09	2.9E-09	3.1E-09	3.2E-09	30.37%	0.84129	
1700	1.4E-09	1.4E-09	1.4E-09	1.5E-09	1.5E-09	1.6E-09	1.6E-09	16.66%	0.47884	
1750	9.2E-10	9.6E-10	1.1E-09	1.2E-09	1.3E-09	1.4E-09	1.5E-09	58.00%	0.86225	
1800	7.8E-10	8.1E-10	9.2E-10	1E-09	1.1E-09	1.2E-09	1.3E-09	61.61%	0.79983	
1850	7.5E-10	8E-10	9.2E-10	1E-09	1.1E-09	1.2E-09	1.3E-09	78.31%	0.90225	
1900	6.2E-10	6.7E-10	7.5E-10	8.2E-10	8.9E-10	9.6E-10	1E-09	65.64%	0.9633	
1950	5.6E-10	5.9E-10	6.7E-10	7.3E-10	8E-10	8.6E-10	9.3E-10	66.83%	0.89988	

**Table 9** The 10cm debris trend shortened into 5 year snapshots. This includes the percent increase in density from the year 2000 to the year 2030, as well as the goodness of fit value for the measurement of how well the data fit a linear approximation.

These gigantic-by-comparison hunks of space debris occur too infrequent to accurately measure their increase in density. This is especially true below 1000km, where most of them fail to get a value larger than .60 for r^2. There are two regions of space often get consistent enough data to fit a line to it: The 1350km regain and the 2000km region.

		1m								
		Year								
		2000	2005	2010	2015	2020	2025	2030	2000 -> 2030	R^2
	200	2.8E-10	1.9E-10	1.8E-10	1.6E-10	1.4E-10	1.1E-10	8.9E-11	-68.51%	0.09349
	250	1.4E-10	9.1E-11	1.1E-10	1.1E-10	1.1E-10	1.1E-10	1.1E-10	-21.53%	0.00291
altitude in km	300	2.9E-10	3.7E-10	3.8E-10	3.9E-10	4.1E-10	4.2E-10	4.3E-10	48.62%	0.01613
	350	3.8E-10	5.2E-10	6.8E-10	8.2E-10	9.6E-10	1.1E-09	1.2E-09	229.36%	0.65431
	400	6.8E-10	8E-10	9.3E-10	1.1E-09	1.3E-09	1.5E-09	1.7E-09	154.89%	0.65755
	450	1.6E-09	1.8E-09	2.3E-09	2.9E-09	3.4E-09	3.9E-09	4.5E-09	182.84%	0.66274
	500	2.6E-09	2.8E-09	3.1E-09	3.2E-09	3.4E-09	3.5E-09	3.7E-09	39.37%	0.20047
	550	3E-09	2.4E-09	2.1E-09	1.7E-09	1.4E-09	1.1E-09	7.2E-10	-75.87%	0.41568
	600	4.5E-09	4.4E-09	4.4E-09	4.4E-09	4.5E-09	4.5E-09	4.5E-09	0.83%	0.02513
	650	2.4E-09	2.2E-09	2.4E-09	2.4E-09	2.5E-09	2.6E-09	2.6E-09	12.51%	0.13435
	700	2.8E-09	3.5E-09	4.3E-09	5.1E-09	5.9E-09	6.7E-09	7.5E-09	166.01%	0.94863
	750	9.5E-09	8.4E-09	8.3E-09	8E-09	7.7E-09	7.5E-09	7.2E-09	-24.38%	0.14365
	800	5.8E-09	6.1E-09	6.9E-09	7.6E-09	8.3E-09	9E-09	9.7E-09	66.89%	0.82245
	850	4E-09	4.1E-09	4.3E-09	4.5E-09	4.7E-09	4.9E-09	5.1E-09	28.68%	0.83081
	900	4E-09	4.1E-09	4.3E-09	4.4E-09	4.6E-09	4.7E-09	4.9E-09	20.54%	0.85226
	950	1E-08	1.1E-08	1.2E-08	1.3E-08	1.4E-08	1.5E-08	1.7E-08	62.13%	0.97502
	1000	3.6E-09	3.7E-09	3.9E-09	4E-09	4.2E-09	4.4E-09	4.5E-09	26.42%	0.84805
	1050	1.9E-09	2E-09	2.1E-09	2.3E-09	2.4E-09	2.5E-09	2.6E-09	36.44%	0.86951
	1100	1.2E-09	1.1E-09	1.2E-09	1.2E-09	1.2E-09	1.3E-09	1.3E-09	10.06%	0.172
	1150	1.5E-09	1.6E-09	1.7E-09	1.8E-09	2E-09	2.1E-09	2.2E-09	43.88%	0.8512
	1200	8.9E-10	9.4E-10	9.9E-10	1.1E-09	1.1E-09	1.2E-09	1.2E-09	37.56%	0.93423
	1250	1.1E-09	1.2E-09	1.3E-09	1.4E-09	1.6E-09	1.7E-09	1.8E-09	66.22%	0.956
	1300	7.4E-10	8.4E-10	9.6E-10	1.1E-09	1.2E-09	1.2E-09	1.3E-09	81.59%	0.90727
	1350	2E-09	2.2E-09	2.3E-09	2.5E-09	2.6E-09	2.8E-09	2.9E-09	46.37%	0.91851
	1400	5E-09	6.1E-09	7.9E-09	9.4E-09	1.1E-08	1.2E-08	1.4E-08	177.79%	0.92742
	1450	3.4E-09	3.5E-09	3.6E-09	3.7E-09	3.8E-09	3.9E-09	4E-09	20.06%	0.80177
	1500	2.3E-09	2.3E-09	2.4E-09	2.4E-09	2.4E-09	2.5E-09	2.5E-09	10.63%	0.97746
	1550	6.2E-10	6.4E-10	6.6E-10	6.9E-10	7.1E-10	7.3E-10	7.6E-10	22.59%	0.94627
	1600	5.2E-10	5.4E-10	5.8E-10	6E-10	6.3E-10	6.6E-10	6.9E-10	31.35%	0.90562
	1650	7.2E-10	7.4E-10	7.8E-10	8.2E-10	8.5E-10	8.9E-10	9.2E-10	28.60%	0.88154
	1700	2.6E-10	2.8E-10	3.2E-10	3.5E-10	3.7E-10	4E-10	4.3E-10	62.91%	0.88352
	1750	1.8E-10	2.1E-10	2.5E-10	2.9E-10	3.3E-10	3.7E-10	4.1E-10	126.30%	0.95299
	1800	1.5E-10	1.7E-10	2.1E-10	2.3E-10	2.6E-10	2.9E-10	3.2E-10	109.39%	0.88814
	1850	1.6E-10	1.8E-10	2.3E-10	2.6E-10	3E-10	3.4E-10	3.8E-10	141.27%	0.9195
	1900	1.1E-10	1.3E-10	1.4E-10	1.6E-10	1.8E-10	1.9E-10	2.1E-10	86.03%	0.89382
	1950	1.1E-10	1.2E-10	1.4E-10	1.6E-10	1.8E-10	2E-10	2.2E-10	106.69%	0.92248

Table 10 The 1m debris trend shortened into 5 year snapshots. This includes the percent increase in density from the year 2000 to the year 2030, as well as the goodness of fit value for the measurement of how well the data fit a linear approximation.

These massive hunks of trash in the sky are mostly entire dormant safelights and multi-stage rocket parts. The rate of growths is much smaller, but there are extremely good values for  $r^2$  considering how small these densities are. While the level of destruction two dead satellites might cause after colliding with each other is quite large, it has an extremely low probability. The increasing levels of objects around 1mm are a much larger cause for concern because they can damage delicate instruments on satellites. The spike around 1400km is most likely leftover parts from multi-stage rockets while the 800km and 900km are more likely to be dead satellites.

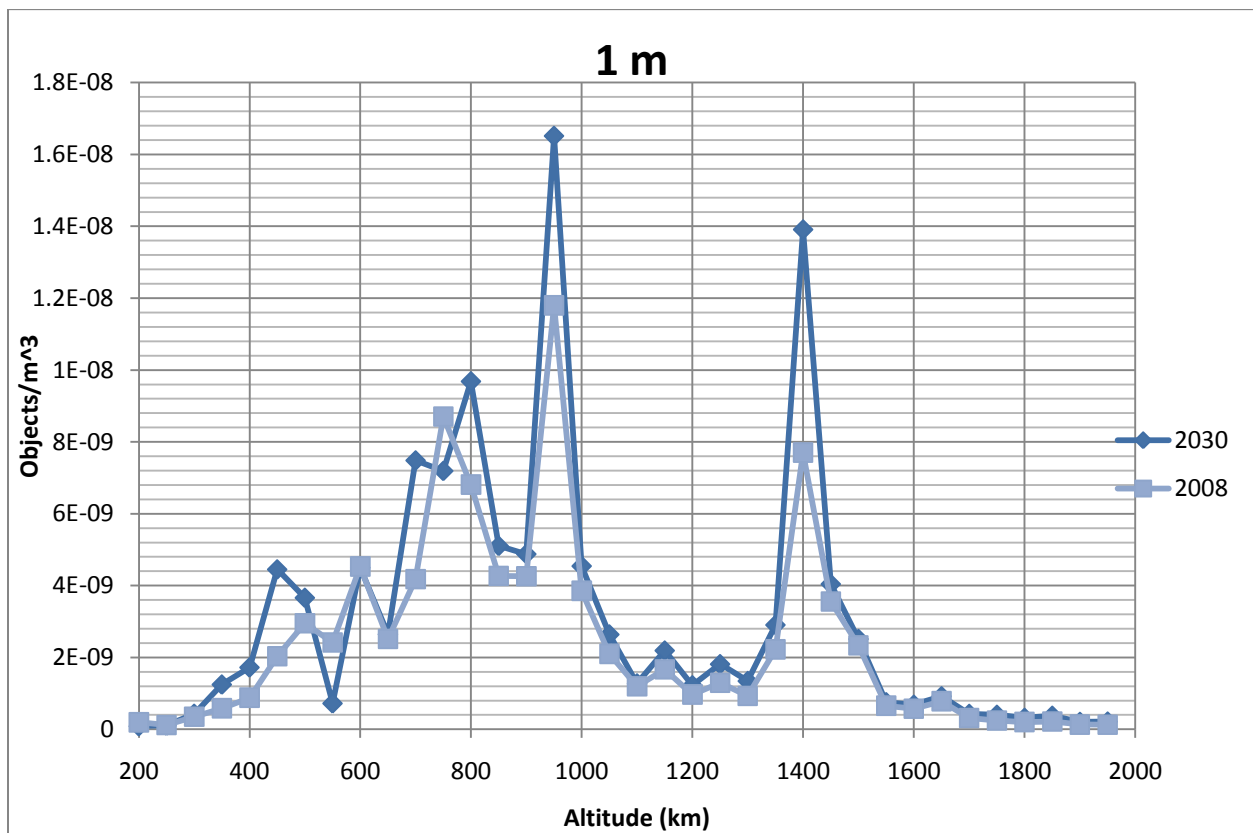


Figure 12 The 1m objects/m³ at 2008 and 2030 from 200km to 1950km.

The last 3 tables contain all the numbers for how the space debris will grow from 2009 to 2030. It includes all 36 altitudes for each of the 6 size groupings.

		10um																					
		2009	2010	2011	2012	2013	2014	2015	2016	2017	2018	2019	2020	2021	2022	2023	2024	2025	2026	2027	2028	2029	2030
200	1.195077	1.275862	1.356648	1.437433	1.518218	1.599003	1.679788	1.760573	1.841359	1.922144	2.002929	2.083714	2.164499	2.245284	2.326069	2.406855	2.487640	2.568425	2.649210	2.729995	2.810780	2.891565	2.972350
250	1.595229	1.677875	1.760521	1.843167	1.925813	2.008458	2.091104	2.173750	2.256396	2.339042	2.421688	2.504334	2.586980	2.669626	2.752272	2.834918	2.917564	3.000210	3.082856	3.165502	3.248148	3.330794	3.413440
300	1.892273	1.9678	2.043328	2.118856	2.194383	2.269911	2.345438	2.420966	2.496494	2.572021	2.647549	2.723077	2.798604	2.874132	2.949660	3.025187	3.100715	3.176242	3.251770	3.327298	3.402825	3.478353	3.553881
350	2.33989	2.443509	2.547129	2.650749	2.754368	2.857988	2.961608	3.065227	3.168847	3.272467	3.376086	3.479706	3.583326	3.686945	3.790565	3.894185	3.997804	4.101424	4.205044	4.308663	4.412283	4.515903	4.619522
400	2.96089	3.110122	3.259354	3.408587	3.557819	3.707051	3.856283	4.005515	4.154747	4.303979	4.453211	4.602443	4.751675	4.900907	5.050139	5.199371	5.348603	5.497835	5.647067	5.796299	5.945531	6.094764	6.243996
450	4.20572	4.455818	4.705916	4.956013	5.206111	5.456208	5.706306	5.956404	6.206502	6.456600	6.706697	6.956795	7.206892	7.456990	7.707088	7.957186	8.207283	8.457381	8.707479	8.957576	9.207674	9.457772	9.707870
450	4.349048	4.601616	4.854185	5.106754	5.359322	5.611891	5.864459	6.117028	6.369596	6.622165	6.874733	7.127302	7.379870	7.632439	7.885007	8.137576	8.390144	8.642712	8.895281	9.147850	9.400418	9.652987	9.905555
550	5.252194	5.58163	5.911066	6.240503	6.569939	6.899376	7.228812	7.558249	7.887685	8.217121	8.546558	8.875994	9.205431	9.534867	9.864304	10.19374	10.52318	10.85261	11.18205	11.51149	11.84093	12.17037	12.50081
600	6.247166	6.662559	7.077952	7.493344	7.908737	8.32413	8.739523	9.154915	9.570308	9.985701	10.40109	10.81649	11.23188	11.64727	12.06266	12.47806	12.89345	13.30884	13.72424	14.13963	14.55502	14.97041	15.38580
650	7.318499	7.811201	8.303904	8.796608	9.289312	9.782016	10.274719	10.767422	11.260125	11.752828	12.245532	12.738235	13.230938	13.723641	14.216344	14.709047	15.201750	15.694453	16.187156	16.679859	17.172562	17.665265	18.157968
700	8.397891	8.95781	9.517729	10.07765	10.63757	11.19749	11.75741	12.31733	12.87725	13.43717	13.99709	14.55701	15.11693	15.67685	16.23677	16.79669	17.35661	17.91653	18.47645	19.03637	19.59629	20.15621	20.71613
750	9.168501	9.754824	10.34115	10.92747	11.51379	12.10012	12.68644	13.27276	13.85908	14.44541	15.03173	15.61805	16.20437	16.79069	17.37702	17.96334	18.54966	19.13598	19.72231	20.30863	20.89496	21.48128	22.06761
800	9.73353	10.32725	10.92097	11.51469	12.10841	12.70213	13.29585	13.88957	14.48329	15.07701	15.67073	16.26445	16.85817	17.45189	18.04561	18.63934	19.23306	19.82678	20.42050	21.01422	21.60794	22.20166	22.79538
850	10.09197	10.6466	11.20122	11.75585	12.31048	12.86511	13.41973	13.97436	14.52899	15.08361	15.63824	16.19287	16.74750	17.30212	17.85675	18.41137	18.96600	19.52063	20.07526	20.62989	21.18452	21.73915	22.29378
900	10.49203	11.01141	11.53079	12.05017	12.56955	13.08892	13.60830	14.12768	14.64706	15.16644	15.68581	16.20519	16.72457	17.24395	17.76333	18.28271	18.80209	19.32147	19.84085	20.36023	20.87961	21.39899	21.91837
950	11.27809	11.78631	12.29453	12.80275	13.31097	13.81919	14.32741	14.83563	15.34385	15.85207	16.36029	16.86852	17.37674	17.88496	18.39318	18.90140	19.40962	19.91784	20.42606	20.93428	21.44250	21.95072	22.45894
1000	12.01255	12.06269	12.52384	12.98498	13.44613	13.90727	14.36842	14.82956	15.29071	15.75185	16.21300	16.67414	17.13528	17.59643	18.05757	18.51872	18.97986	19.44101	19.90215	20.36330	20.82444	21.28559	21.74673
1000	10.4204	12.87486	13.32932	13.78379	14.23825	14.69271	15.14717	15.60163	16.05610	16.51056	16.96502	17.41948	17.87394	18.32841	18.78287	19.23733	19.69179	20.14625	20.60071	21.05518	21.50964	21.96411	22.41857
1100	13.26369	13.69126	14.11884	14.54641	14.97399	15.40156	15.82914	16.25671	16.68428	17.11186	17.53943	17.96700	18.39458	18.82216	19.24973	19.67731	20.10488	20.53246	20.96003	21.38761	21.81518	22.24275	22.67033
1150	13.84364	14.20218	14.56073	14.91928	15.27783	15.63638	15.99493	16.35347	16.71202	17.07057	17.42912	17.78767	18.14622	18.50477	18.86331	19.22186	19.58041	19.93896	20.29751	20.65606	21.01461	21.37315	21.73170
1200	14.94466	14.23257	14.52047	14.80838	15.09629	15.38419	15.67210	15.96001	16.24791	16.53581	16.82372	17.11162	17.39953	17.68743	17.97534	18.26324	18.55115	18.83906	19.12697	19.41488	19.70279	19.99070	20.27861
1250	13.77742	14.01742	14.25741	14.49741	14.73739	14.97738	15.21738	15.45737	15.69736	15.93735	16.17734	16.41733	16.65733	16.89732	17.13731	17.37731	17.61730	17.85729	18.09728	18.33727	18.57726	18.81725	19.05724
1300	13.21085	13.42673	13.64261	13.85850	14.07438	14.29026	14.50615	14.72203	14.93791	15.15380	15.36968	15.58556	15.80144	16.01733	16.23321	16.44909	16.66498	16.88086	17.09674	17.31262	17.52851	17.74440	17.96028
1350	12.86433	13.07349	13.28265	13.49181	13.70096	13.91012	14.11928	14.32844	14.53760	14.74675	14.95591	15.16507	15.37423	15.58339	15.79255	16.00171	16.21086	16.42002	16.62918	16.83834	17.04750	17.25666	17.46582
1400	12.72941	12.96182	13.19422	13.42663	13.65904	13.89144	14.12385	14.35626	14.58866	14.82107	15.05348	15.28588	15.51829	15.75070	15.98311	16.21551	16.44792	16.68033	16.91274	17.14515	17.37756	17.60997	17.84238
1450	12.94441	13.23072	13.51702	13.80332	14.08962	14.37592	14.66223	14.94853	15.23483	15.52113	15.80743	16.09374	16.38004	16.66634	16.95264	17.23895	17.52525	17.81155	18.09785	18.38415	18.67046	18.95676	19.24307
1500	11.49862	11.82357	12.14852	12.47347	12.79843	13.12338	13.44833	13.77328	14.09823	14.42318	14.74814	15.07309	15.39804	15.72299	16.04794	16.37289	16.69784	17.02279	17.34774	17.67269	17.99764	18.32259	18.64754
1500	10.46442	10.80481	11.14521	11.48561	11.826	12.1664	12.5068	12.84719	13.18759	13.52799	13.86838	14.20878	14.54918	14.88957	15.22997	15.57037	15.91076	16.25116	16.59156	16.93195	17.27235	17.61275	17.95315
1600	9.812899	10.15908	10.50527	10.85145	11.19764	11.54383	11.89001	12.23620	12.58238	12.92857	13.27475	13.62094	13.96713	14.31331	14.65949	15.00568	15.35187	15.69806	16.04425	16.39044	16.73663	17.08282	17.42901
1650	9.170714	9.515158	9.859601	10.20405	10.54849	10.89293	11.23738	11.58182	11.92626	12.27071	12.61515	12.95960	13.30404	13.64848	13.99293	14.33737	14.68182	15.02626	15.37071	15.71515	16.05960	16.40405	16.74849
1700	8.616568	8.963766	9.310964	9.658163	10.005362	10.352561	10.699760	11.046959	11.394158	11.741357	12.088556	12.435755	12.782954	13.130153	13.477352	13.824551	14.171750	14.518949	14.866148	15.213347	15.560546	15.907745	16.254944
1750	8.419991	8.776571	9.133151	9.489731	9.846311	10.202891	10.559471	10.916051	11.272631	11.629211	11.985791	12.342371	12.698951	13.055531	13.412111	13.768691	14.125271	14.481851	14.838431	15.195011	15.551591	15.908171	16.264751
1800	8.148278	8.496556	8.844835	9.193113	9.541392	9.889671	10.237950	10.586230	10.934510	11.282790	11.631070	11.979350	12.327630	12.675910	13.024190	13.372470	13.720750	14.069030	14.417310	14.765590	15.113870	15.462150	15.810430
1850	7.887512	8.226277	8.565042	8.903807	9.242572	9.581337	9.920102	10.258867	10.597632	10.936397	11.275162	11.613927	11.952692	12.291457	12.630222	12.968987	13.307752	13.646517	13.985282	14.324047	14.662812	15.001577	15.340342
1900	7.698743	8.012955	8.327167	8.641378	8.955590	9.269802	9.584014	9.898226	10.212438	10.526650	10.840862	11.155074	11.469286	11.783498	12.097710	12.411922	12.726134	13.040346	13.354558	13.668770	13.982982	14.297194	14.611406
1950	7.487829	7.786502	8.085175	8.383848	8.682521	8.981195	9.279868	9.578541	9.877214	10.175887	10.474560	10.773233	11.071906	11.370579	11.669252	11.967925	12.266598	12.565271	12.863944	13.162617	13.461290	13.759963	14.058636

		100um																					
		2009	2010	2011	2012	2013	2014	2015	2016	2017	2018	2019	2020	2021	2022	2023	2024	2025	2026	2027	2028	2029	2030
200	0.024463	0.025884	0.027304	0.028724	0.030145	0.031565	0.032986	0.034406	0.035826	0.037247	0.038667	0.040088	0.041508	0.042929	0.044349	0.045769	0.047189	0.048610	0.050030	0.051451	0.052871	0.054292	0.055713
250	0.041775	0.042763	0.043751	0.044739	0.045727	0.046715	0.047703	0.048691	0.049679	0.05													



		1mm																					
		2009	2010	2011	2012	2013	2014	2015	2016	2017	2018	2019	2020	2021	2022	2023	2024	2025	2026	2027	2028	2029	2030
200	5.93E-05	6.28E-05	6.64E-05	7E-05	7.35E-05	7.71E-05	8.07E-05	8.43E-05	8.78E-05	9.14E-05	9.50E-05	9.85E-05	0.000102	0.000106	0.000109	0.000113	0.000116	0.00012	0.000124	0.000127	0.000131	0.000134	0.000138
250	5.24E-05	5.45E-05	5.66E-05	5.87E-05	6.08E-05	6.29E-05	6.50E-05	6.71E-05	6.92E-05	7.13E-05	7.34E-05	7.55E-05	7.76E-05	7.97E-05	8.18E-05	8.4E-05	8.61E-05	8.82E-05	9.03E-05	9.24E-05	9.45E-05	9.66E-05	9.87E-05
300	9.27E-05	9.54E-05	9.81E-05	0.000101	0.000104	0.000106	0.000109	0.000112	0.000115	0.000117	0.00012	0.000123	0.000125	0.000128	0.000131	0.000134	0.000136	0.000139	0.000142	0.000145	0.000147	0.00015	0.000153
350	0.000134	0.000138	0.000142	0.000146	0.00015	0.000154	0.000158	0.000162	0.000166	0.00017	0.000174	0.000178	0.000182	0.000186	0.00019	0.000195	0.000199	0.000203	0.000207	0.000211	0.000215	0.000219	0.000223
400	0.000172	0.000178	0.000184	0.00019	0.000196	0.000202	0.000207	0.000213	0.000219	0.000225	0.000231	0.000237	0.000242	0.000248	0.000254	0.00026	0.000266	0.000272	0.000277	0.000283	0.000289	0.000295	0.000301
450	0.000261	0.000271	0.000281	0.000291	0.000301	0.000311	0.000321	0.000331	0.000341	0.000351	0.000361	0.000371	0.000381	0.000391	0.000401	0.000411	0.000421	0.000431	0.000441	0.000451	0.000461	0.000471	0.000481
500	0.000315	0.000327	0.000339	0.000351	0.000363	0.000375	0.000387	0.000399	0.000411	0.000423	0.000435	0.000447	0.000459	0.000471	0.000482	0.000494	0.000506	0.000518	0.00053	0.000542	0.000554	0.000566	0.000578
550	0.00037	0.000387	0.000403	0.000419	0.000436	0.000452	0.000468	0.000485	0.000501	0.000517	0.000534	0.00055	0.000566	0.000583	0.000599	0.000615	0.000632	0.000648	0.000664	0.000681	0.000697	0.000713	0.000729
600	0.000433	0.000453	0.000473	0.000493	0.000513	0.000533	0.000553	0.000573	0.000593	0.000614	0.000634	0.000654	0.000674	0.000694	0.000714	0.000734	0.000754	0.000774	0.000794	0.000814	0.000834	0.000855	0.000875
650	0.00051	0.000536	0.000561	0.000586	0.000611	0.000636	0.000661	0.000686	0.000711	0.000736	0.000762	0.000787	0.000812	0.000837	0.000862	0.000887	0.000912	0.000937	0.000963	0.000988	0.001013	0.001038	0.001063
700	0.000565	0.000592	0.00062	0.000647	0.000675	0.000702	0.00073	0.000757	0.000785	0.000812	0.000839	0.000867	0.000894	0.000922	0.000949	0.000977	0.001004	0.001032	0.001059	0.001087	0.001114	0.001142	0.001169
750	0.000654	0.000684	0.000714	0.000744	0.000775	0.000805	0.000835	0.000865	0.000895	0.000925	0.000955	0.000986	0.001016	0.001046	0.001076	0.001106	0.001136	0.001167	0.001197	0.001227	0.001257	0.001287	0.001317
800	0.000745	0.000775	0.000805	0.000835	0.000865	0.000895	0.000925	0.000955	0.000985	0.001015	0.001045	0.001075	0.001105	0.001135	0.001165	0.001195	0.001225	0.001255	0.001285	0.001315	0.001345	0.001375	0.001405
850	0.000836	0.000866	0.000896	0.000926	0.000956	0.000986	0.001016	0.001046	0.001076	0.001106	0.001136	0.001166	0.001196	0.001226	0.001256	0.001286	0.001316	0.001346	0.001376	0.001406	0.001436	0.001466	0.001496
900	0.000927	0.000957	0.000987	0.001017	0.001047	0.001077	0.001107	0.001137	0.001167	0.001197	0.001227	0.001257	0.001287	0.001317	0.001347	0.001377	0.001407	0.001437	0.001467	0.001497	0.001527	0.001557	0.001587
950	0.001018	0.001048	0.001078	0.001108	0.001138	0.001168	0.001198	0.001228	0.001258	0.001288	0.001318	0.001348	0.001378	0.001408	0.001438	0.001468	0.001498	0.001528	0.001558	0.001588	0.001618	0.001648	0.001678
1000	0.001109	0.001139	0.001169	0.001199	0.001229	0.001259	0.001289	0.001319	0.001349	0.001379	0.001409	0.001439	0.001469	0.001499	0.001529	0.001559	0.001589	0.001619	0.001649	0.001679	0.001709	0.001739	0.001769
1050	0.001200	0.001230	0.001260	0.001290	0.001320	0.001350	0.001380	0.001410	0.001440	0.001470	0.001500	0.001530	0.001560	0.001590	0.001620	0.001650	0.001680	0.001710	0.001740	0.001770	0.001800	0.001830	0.001860
1100	0.001291	0.001321	0.001351	0.001381	0.001411	0.001441	0.001471	0.001501	0.001531	0.001561	0.001591	0.001621	0.001651	0.001681	0.001711	0.001741	0.001771	0.001801	0.001831	0.001861	0.001891	0.001921	0.001951
1150	0.001382	0.001412	0.001442	0.001472	0.001502	0.001532	0.001562	0.001592	0.001622	0.001652	0.001682	0.001712	0.001742	0.001772	0.001802	0.001832	0.001862	0.001892	0.001922	0.001952	0.001982	0.002012	0.002042
1200	0.001473	0.001503	0.001533	0.001563	0.001593	0.001623	0.001653	0.001683	0.001713	0.001743	0.001773	0.001803	0.001833	0.001863	0.001893	0.001923	0.001953	0.001983	0.002013	0.002043	0.002073	0.002103	0.002133
1250	0.001564	0.001594	0.001624	0.001654	0.001684	0.001714	0.001744	0.001774	0.001804	0.001834	0.001864	0.001894	0.001924	0.001954	0.001984	0.002014	0.002044	0.002074	0.002104	0.002134	0.002164	0.002194	0.002224
1300	0.001655	0.001685	0.001715	0.001745	0.001775	0.001805	0.001835	0.001865	0.001895	0.001925	0.001955	0.001985	0.002015	0.002045	0.002075	0.002105	0.002135	0.002165	0.002195	0.002225	0.002255	0.002285	0.002315
1350	0.001746	0.001776	0.001806	0.001836	0.001866	0.001896	0.001926	0.001956	0.001986	0.002016	0.002046	0.002076	0.002106	0.002136	0.002166	0.002196	0.002226	0.002256	0.002286	0.002316	0.002346	0.002376	0.002406
1400	0.001837	0.001867	0.001897	0.001927	0.001957	0.001987	0.002017	0.002047	0.002077	0.002107	0.002137	0.002167	0.002197	0.002227	0.002257	0.002287	0.002317	0.002347	0.002377	0.002407	0.002437	0.002467	0.002497
1450	0.001928	0.001958	0.001988	0.002018	0.002048	0.002078	0.002108	0.002138	0.002168	0.002198	0.002228	0.002258	0.002288	0.002318	0.002348	0.002378	0.002408	0.002438	0.002468	0.002498	0.002528	0.002558	0.002588
1500	0.002019	0.002049	0.002079	0.002109	0.002139	0.002169	0.002199	0.002229	0.002259	0.002289	0.002319	0.002349	0.002379	0.002409	0.002439	0.002469	0.002499	0.002529	0.002559	0.002589	0.002619	0.002649	0.002679
1550	0.002110	0.002140	0.002170	0.002200	0.002230	0.002260	0.002290	0.002320	0.002350	0.002380	0.002410	0.002440	0.002470	0.002500	0.002530	0.002560	0.002590	0.002620	0.002650	0.002680	0.002710	0.002740	0.002770
1600	0.002201	0.002231	0.002261	0.002291	0.002321	0.002351	0.002381	0.002411	0.002441	0.002471	0.002501	0.002531	0.002561	0.002591	0.002621	0.002651	0.002681	0.002711	0.002741	0.002771	0.002801	0.002831	0.002861
1650	0.002292	0.002322	0.002352	0.002382	0.002412	0.002442	0.002472	0.002502	0.002532	0.002562	0.002592	0.002622	0.002652	0.002682	0.002712	0.002742	0.002772	0.002802	0.002832	0.002862	0.002892	0.002922	0.002952
1700	0.002383	0.002413	0.002443	0.002473	0.002503	0.002533	0.002563	0.002593	0.002623	0.002653	0.002683	0.002713	0.002743	0.002773	0.002803	0.002833	0.002863	0.002893	0.002923	0.002953	0.002983	0.003013	0.003043
1750	0.002474	0.002504	0.002534	0.002564	0.002594	0.002624	0.002654	0.002684	0.002714	0.002744	0.002774	0.002804	0.002834	0.002864	0.002894	0.002924	0.002954	0.002984	0.003014	0.003044	0.003074	0.003104	0.003134
1800	0.002565	0.002595	0.002625	0.002655	0.002685	0.002715	0.002745	0.002775	0.002805	0.002835	0.002865	0.002895	0.002925	0.002955	0.002985	0.003015	0.003045	0.003075	0.003105	0.003135	0.003165	0.003195	0.003225
1850	0.002656	0.002686	0.002716	0.002746	0.002776	0.002806	0.002836	0.002866	0.002896	0.002926	0.002956	0.002986	0.003016	0.003046	0.003076	0.003106	0.003136	0.003166	0.003196	0.003226	0.003256	0.003286	0.003316
1900	0.002747	0.002777	0.002807	0.002837	0.002867	0.002897	0.002927	0.002957	0.002987	0.003017	0.003047	0.003077	0.003107	0.003137	0.003167	0.003197	0.003227	0.003257	0.003287	0.003317	0.003347	0.003377	0.003407
1950	0.002838	0.002868	0.002898	0.002928	0.002958	0.002988	0.003018	0.003048	0.003078	0.003108	0.003138	0.003168	0.003198	0.003228	0.003258	0.003288	0.003318	0.003348	0.003378	0.003408	0.003438	0.003468	0.003498

		1cm																					
		2009	2010	2011	2012	2013	2014	2015	2016	2017	2018	2019	2020	2021	2022	2023	2024	2025	2026	2027	2028	2029	2030
200	4.65E-09	4.96E-09	5.28E-09	5.6E-09	5.91E-09	6.23E-09	6.55E-09	6.87E-09	7.18E-09	7.5E-09	7.82E-09	8.14E-09	8.45E-09	8.77E-09	9.09E-09	9.41E-09	9.72E-09	1E-08	1.04E-08	1.07E-08	1.1E-08	1.13E-08	1.16E-08
250	1.93E-09	2.02E-09	2.12E-09	2.21E-09	2.3E-09	2.39E-09	2.49E-09	2.58E-09	2.67E-09	2.77E-09	2.86E-09	2.95E-09	3.04E-09	3.14E-09	3.23E-09	3.32E-09	3.41E-09	3.51E-09	3.6E-09	3.69E-09	3.78E-09	3.88E-	

		10cm																					
		2009	2010	2011	2012	2013	2014	2015	2016	2017	2018	2019	2020	2021	2022	2023	2024	2025	2026	2027	2028	2029	2030
200	3.33E-10	3.35E-10	3.38E-10	3.4E-10	3.42E-10	3.45E-10	3.47E-10	3.49E-10	3.52E-10	3.54E-10	3.56E-10	3.59E-10	3.61E-10	3.63E-10	3.66E-10	3.68E-10	3.7E-10	3.73E-10	3.75E-10	3.77E-10	3.8E-10	3.82E-10	
250	2.37E-10	2.39E-10	2.41E-10	2.43E-10	2.45E-10	2.47E-10	2.49E-10	2.51E-10	2.53E-10	2.55E-10	2.57E-10	2.59E-10	2.61E-10	2.63E-10	2.65E-10	2.67E-10	2.7E-10	2.73E-10	2.75E-10	2.77E-10	2.79E-10	2.82E-10	
300	1.74E-10	1.74E-10	7.73E-10	8.03E-10	8.32E-10	8.62E-10	8.91E-10	9.21E-10	9.5E-10	9.8E-10	1.01E-09	1.04E-09	1.07E-09	1.1E-09	1.13E-09	1.16E-09	1.19E-09	1.22E-09	1.24E-09	1.27E-09	1.3E-09	1.33E-09	
350	1.38E-09	1.44E-09	1.5E-09	1.56E-09	1.62E-09	1.68E-09	1.74E-09	1.8E-09	1.85E-09	1.91E-09	1.97E-09	2.03E-09	2.09E-09	2.15E-09	2.21E-09	2.27E-09	2.32E-09	2.38E-09	2.44E-09	2.5E-09	2.56E-09	2.62E-09	
400	1.85E-09	1.92E-09	1.99E-09	2.06E-09	2.13E-09	2.2E-09	2.27E-09	2.34E-09	2.42E-09	2.49E-09	2.56E-09	2.63E-09	2.7E-09	2.77E-09	2.84E-09	2.91E-09	2.99E-09	3.06E-09	3.13E-09	3.2E-09	3.27E-09	3.34E-09	
450	3.77E-09	3.95E-09	4.14E-09	4.32E-09	4.5E-09	4.68E-09	4.87E-09	5.05E-09	5.23E-09	5.41E-09	5.6E-09	5.78E-09	5.96E-09	6.15E-09	6.33E-09	6.51E-09	6.69E-09	6.88E-09	7.06E-09	7.24E-09	7.42E-09	7.61E-09	
500	6.02E-09	6.15E-09	6.29E-09	6.42E-09	6.55E-09	6.68E-09	6.81E-09	6.95E-09	7.08E-09	7.21E-09	7.34E-09	7.48E-09	7.61E-09	7.74E-09	7.87E-09	8.01E-09	8.14E-09	8.27E-09	8.4E-09	8.54E-09	8.67E-09	8.8E-09	
550	6.07E-09	6.1E-09	6.13E-09	6.15E-09	6.18E-09	6.21E-09	6.24E-09	6.27E-09	6.3E-09	6.33E-09	6.36E-09	6.38E-09	6.41E-09	6.44E-09	6.47E-09	6.5E-09	6.53E-09	6.56E-09	6.59E-09	6.61E-09	6.64E-09	6.67E-09	
600	9.01E-09	9.09E-09	9.17E-09	9.25E-09	9.33E-09	9.41E-09	9.48E-09	9.56E-09	9.64E-09	9.72E-09	9.8E-09	9.87E-09	9.95E-09	1E-08	1.01E-08	1.02E-08	1.03E-08	1.03E-08	1.04E-08	1.05E-08	1.06E-08	1.07E-08	
650	7.76E-09	7.77E-09	7.78E-09	7.8E-09	7.81E-09	7.83E-09	7.84E-09	7.86E-09	7.87E-09	7.89E-09	7.9E-09	7.91E-09	7.93E-09	7.94E-09	7.96E-09	7.97E-09	7.99E-09	8E-09	8.01E-09	8.03E-09	8.04E-09	8.06E-09	
700	1.17E-08	1.2E-08	1.23E-08	1.26E-08	1.3E-08	1.33E-08	1.36E-08	1.39E-08	1.42E-08	1.45E-08	1.49E-08	1.52E-08	1.55E-08	1.58E-08	1.61E-08	1.64E-08	1.68E-08	1.71E-08	1.74E-08	1.77E-08	1.8E-08	1.83E-08	
750	1.91E-08	1.93E-08	1.94E-08	1.96E-08	1.98E-08	2E-08	2.01E-08	2.03E-08	2.05E-08	2.07E-08	2.08E-08	2.1E-08	2.12E-08	2.14E-08	2.15E-08	2.17E-08	2.19E-08	2.21E-08	2.23E-08	2.24E-08	2.26E-08	2.28E-08	
800	1.73E-08	1.75E-08	1.78E-08	1.8E-08	1.83E-08	1.85E-08	1.88E-08	1.9E-08	1.93E-08	1.95E-08	1.98E-08	2E-08	2.03E-08	2.05E-08	2.08E-08	2.11E-08	2.13E-08	2.16E-08	2.18E-08	2.21E-08	2.23E-08	2.26E-08	
850	1.47E-08	1.48E-08	1.5E-08	1.51E-08	1.52E-08	1.53E-08	1.55E-08	1.56E-08	1.57E-08	1.58E-08	1.6E-08	1.61E-08	1.62E-08	1.64E-08	1.65E-08	1.66E-08	1.67E-08	1.69E-08	1.7E-08	1.71E-08	1.72E-08	1.74E-08	
900	1.67E-08	1.69E-08	1.71E-08	1.73E-08	1.75E-08	1.77E-08	1.79E-08	1.81E-08	1.83E-08	1.85E-08	1.87E-08	1.89E-08	1.91E-08	1.93E-08	1.95E-08	1.97E-08	1.99E-08	2.01E-08	2.03E-08	2.05E-08	2.07E-08	2.09E-08	
950	2.58E-08	2.64E-08	2.7E-08	2.75E-08	2.81E-08	2.87E-08	2.92E-08	2.98E-08	3.04E-08	3.09E-08	3.15E-08	3.21E-08	3.26E-08	3.32E-08	3.38E-08	3.44E-08	3.49E-08	3.55E-08	3.61E-08	3.66E-08	3.72E-08	3.78E-08	
1000	1.4E-08	1.42E-08	1.44E-08	1.46E-08	1.48E-08	1.5E-08	1.52E-08	1.54E-08	1.56E-08	1.58E-08	1.6E-08	1.62E-08	1.64E-08	1.66E-08	1.68E-08	1.7E-08	1.72E-08	1.74E-08	1.76E-08	1.78E-08	1.8E-08	1.82E-08	
1050	9.5E-09	9.53E-09	9.55E-09	9.57E-09	9.59E-09	9.61E-09	9.63E-09	9.65E-09	9.68E-09	9.7E-09	9.72E-09	9.74E-09	9.76E-09	9.78E-09	9.8E-09	9.83E-09	9.85E-09	9.87E-09	9.89E-09	9.91E-09	9.93E-09	9.95E-09	
1100	6.18E-09	6.21E-09	6.25E-09	6.28E-09	6.31E-09	6.34E-09	6.37E-09	6.4E-09	6.43E-09	6.47E-09	6.5E-09	6.53E-09	6.56E-09	6.59E-09	6.62E-09	6.65E-09	6.68E-09	6.72E-09	6.75E-09	6.78E-09	6.81E-09	6.84E-09	
1150	4.68E-09	4.73E-09	4.78E-09	4.83E-09	4.88E-09	4.93E-09	4.98E-09	5.02E-09	5.07E-09	5.12E-09	5.17E-09	5.22E-09	5.27E-09	5.32E-09	5.37E-09	5.41E-09	5.46E-09	5.51E-09	5.56E-09	5.61E-09	5.66E-09	5.71E-09	
1200	3.6E-09	3.68E-09	3.76E-09	3.84E-09	3.92E-09	4E-09	4.08E-09	4.16E-09	4.24E-09	4.32E-09	4.4E-09	4.48E-09	4.56E-09	4.64E-09	4.71E-09	4.79E-09	4.87E-09	4.95E-09	5.03E-09	5.11E-09	5.19E-09	5.27E-09	
1250	6.28E-09	6.46E-09	6.63E-09	6.81E-09	6.98E-09	7.16E-09	7.33E-09	7.51E-09	7.68E-09	7.86E-09	8.03E-09	8.21E-09	8.39E-09	8.56E-09	8.74E-09	8.91E-09	9.09E-09	9.26E-09	9.44E-09	9.61E-09	9.79E-09	9.96E-09	
1300	4.38E-09	4.46E-09	4.55E-09	4.63E-09	4.72E-09	4.8E-09	4.89E-09	4.97E-09	5.06E-09	5.14E-09	5.23E-09	5.31E-09	5.39E-09	5.48E-09	5.56E-09	5.65E-09	5.73E-09	5.82E-09	5.9E-09	5.99E-09	6.07E-09	6.16E-09	
1350	6.13E-09	6.26E-09	6.4E-09	6.53E-09	6.66E-09	6.8E-09	6.93E-09	7.07E-09	7.2E-09	7.34E-09	7.47E-09	7.61E-09	7.74E-09	7.88E-09	8.01E-09	8.15E-09	8.28E-09	8.41E-09	8.55E-09	8.68E-09	8.82E-09	8.95E-09	
1400	1.46E-08	1.5E-08	1.55E-08	1.59E-08	1.64E-08	1.68E-08	1.73E-08	1.77E-08	1.81E-08	1.86E-08	1.9E-08	1.95E-08	1.99E-08	2.04E-08	2.08E-08	2.13E-08	2.17E-08	2.22E-08	2.26E-08	2.3E-08	2.35E-08	2.39E-08	
1450	1.29E-08	1.3E-08	1.32E-08	1.33E-08	1.34E-08	1.35E-08	1.37E-08	1.38E-08	1.39E-08	1.4E-08	1.41E-08	1.43E-08	1.44E-08	1.45E-08	1.46E-08	1.48E-08	1.49E-08	1.5E-08	1.51E-08	1.53E-08	1.54E-08	1.55E-08	
1500	7.44E-09	7.47E-09	7.49E-09	7.52E-09	7.55E-09	7.58E-09	7.61E-09	7.63E-09	7.66E-09	7.69E-09	7.72E-09	7.75E-09	7.77E-09	7.8E-09	7.83E-09	7.86E-09	7.89E-09	7.91E-09	7.94E-09	7.97E-09	8E-09	8.03E-09	
1550	3.49E-09	3.52E-09	3.56E-09	3.6E-09	3.63E-09	3.67E-09	3.7E-09	3.74E-09	3.77E-09	3.81E-09	3.84E-09	3.88E-09	3.91E-09	3.95E-09	3.98E-09	4.02E-09	4.05E-09	4.09E-09	4.12E-09	4.16E-09	4.19E-09	4.23E-09	
1600	2.7E-09	2.72E-09	2.75E-09	2.78E-09	2.81E-09	2.84E-09	2.87E-09	2.89E-09	2.92E-09	2.95E-09	2.98E-09	3.01E-09	3.04E-09	3.06E-09	3.09E-09	3.12E-09	3.15E-09	3.18E-09	3.21E-09	3.23E-09	3.26E-09	3.29E-09	
1650	2.64E-09	2.67E-09	2.69E-09	2.72E-09	2.74E-09	2.77E-09	2.8E-09	2.82E-09	2.85E-09	2.87E-09	2.9E-09	2.93E-09	2.95E-09	2.98E-09	3E-09	3.03E-09	3.05E-09	3.08E-09	3.11E-09	3.13E-09	3.16E-09	3.18E-09	
1700	1.43E-09	1.44E-09	1.45E-09	1.46E-09	1.47E-09	1.48E-09	1.48E-09	1.49E-09	1.5E-09	1.51E-09	1.52E-09	1.53E-09	1.54E-09	1.55E-09	1.56E-09	1.57E-09	1.58E-09	1.59E-09	1.6E-09	1.61E-09	1.62E-09	1.61E-09	
1750	1.06E-09	1.08E-09	1.1E-09	1.12E-09	1.13E-09	1.15E-09	1.17E-09	1.19E-09	1.21E-09	1.23E-09	1.25E-09	1.27E-09	1.28E-09	1.3E-09	1.32E-09	1.34E-09	1.36E-09	1.38E-09	1.4E-09	1.42E-09	1.43E-09	1.45E-09	
1800	9.08E-10	9.25E-10	9.42E-10	9.59E-10	9.76E-10	9.93E-10	1.01E-09	1.03E-09	1.04E-09	1.06E-09	1.08E-09	1.1E-09	1.11E-09	1.13E-09	1.15E-09	1.16E-09	1.18E-09	1.2E-09	1.21E-09	1.23E-09	1.25E-09	1.27E-09	
1850	9.03E-10	9.23E-10	9.44E-10	9.65E-10	9.85E-10	1.01E-09	1.03E-09	1.05E-09	1.07E-09	1.09E-09	1.11E-09	1.13E-09	1.15E-09	1.17E-09	1.19E-09	1.21E-09	1.23E-09	1.25E-09	1.27E-09	1.29E-09	1.32E-09	1.34E-09	
1900	7.41E-10	7.55E-10	7.69E-10	7.83E-10	7.97E-10	8.1E-10	8.24E-10	8.38E-10	8.52E-10	8.66E-10	8.8E-10	8.94E-10	9.08E-10	9.22E-10	9.35E-10	9.49E-10	9.63E-10	9.77E-10	9.91E-10	1E-09	1.02E-09	1.03E-09	
1950	6.57E-10	6.7E-10	6.83E-10	6.96E-10	7.09E-10	7.22E-10	7.35E-10	7.47E-10	7.6E-10	7.73E-10	7.86E-10	7.99E-10	8.12E-10	8.25E-10	8.37E-10	8.5E-10	8.63E-10	8.76E-10	8.89E-10	9.02E-10	9.15E-10	9.28E-10	
		1m																					
		2009	2010	2011	2012	2013	2014	2015	2016	2017	2018	2019	2020	2021	2022	2023	2024	2025	2026	2027	2028	2029	2030
200	1.86E-10	1.82E-10	1.77E-10	1.72E-10	1.68E-10	1.63E-10	1.58E-10	1.54E-10	1.49E-10	1.45E-10	1.4E-10	1.35E-10	1.31E-10	1.26E-10	1.21E-10	1.17E-10	1.12E-10	1.07E-10	1.03E-10	9.82E-11	9.36E-11	8.89E-11	
250	1.14E-10	1.13E-10	1.13E-10	1.13E-10	1.12E-10	1.12E-10	1.11E-10	1.11E-10	1.11E-10	1.1E-10	1.1E-10	1.1E-10	1.09E-10	1.09E-10	1.09E-10	1.08E-10	1.08E-10	1.08E-10	1.07E-10	1.07E-10	1.06E-10	1.06E-10	
300	3.78E-10	3.81E-10	3.83E-10	3.86E-10	3.89E-10	3.91E-10	3.94E-10	3.97E-10	3.99E-10	4.02E-10	4.05E-10	4.08E-10	4.1E-10	4.13E-10	4.15E-10	4.18E-10	4.21E-10	4.23E-10	4.26E-10	4.29E-10	4.32E-10	4.34E-10	
350	6.51E-10	6.79E-10	7.08E-10	7.36E-10	7.65E-10	7.93E-10	8.21E-10	8.5E-10	8.78E-10	9.07E-10	9.35E-10	9.64E-10	9.92E-10	1.02E-09	1.05E-09	1.08E-09	1.11E-09	1.13E-09	1.16E-09	1.19E-09	1.22E-0		

## Conclusion

The intent of this thesis was to learn how much space debris there is around the earth, where it is located, and how fast it is growing. The debris is located in 3 major regions. The first is the large band around the equator that dominates the 200km to 500km region. The second and third are the clusters at the North Pole and the South Pole, which are significant past 600km until falling off at around 1500km.

That rate of growth is alarming in many populated regions of LEO. The 100µm data around 900km show a 655% increase with a  $r^2$  of .93. The 600km to 1200km region in general shows strong levels of increase. This is a region of space that is both heavily populated by satellites, and has extremely long orbital decay periods. The 200km to 400km data show heavy increases that are not linear. While this lower region of space will clean itself up fairly quickly due to the extremely short orbital decay time, it is evidence that we are not currently doing enough to limit the spread of debris into the LEO region of space.

	10um	r^2	100um	r^2	1mm	r^2	1cm	r^2	10cm	r^2	1m	r^2
200	387.17%	0.7301776	282.05%	0.74474652	319.24%	0.81160737	1359.21%	0.455585	7.41%	0.0168	-68.51%	0.09349481
250	230.34%	0.66507586	73.86%	0.41277301	156.87%	0.69060516	359.63%	0.44676	-3.60%	0.0118	-21.53%	0.00290877
300	174.44%	0.67939304	79.53%	0.40928875	112.24%	0.60050417	499.48%	0.764348	248.15%	0.5234	48.62%	0.01612932
350	211.82%	0.75261892	89.65%	0.48753144	115.87%	0.62794303	429.50%	0.951017	190.94%	0.7584	229.36%	0.654309
400	245.41%	0.79432706	113.94%	0.70715044	128.64%	0.78511542	495.06%	0.856757	114.36%	0.5078	154.89%	0.65755056
450	318.66%	0.80975628	134.35%	0.74171409	141.41%	0.79167352	420.42%	0.883048	185.99%	0.6666	182.84%	0.66273869
500	296.65%	0.80030028	172.89%	0.73459283	137.30%	0.7615764	323.05%	0.873618	71.12%	0.5612	39.37%	0.20047318
550	332.62%	0.82249207	336.74%	0.73975856	171.78%	0.767076	140.64%	0.541478	-2.98%	0.0088	-75.87%	0.41568176
600	367.30%	0.8459843	372.68%	0.74887836	189.17%	0.79009123	240.05%	0.801594	23.79%	0.275	0.83%	0.02512531
650	368.30%	0.85187629	518.92%	0.7413987	210.83%	0.80825896	164.81%	0.879172	-7.39%	0.004	12.51%	0.13434869
700	357.50%	0.85330306	543.61%	0.79864588	211.76%	0.83923142	137.69%	0.875994	100.33%	0.8487	166.01%	0.94863137
750	328.70%	0.8485424	469.17%	0.81551954	195.87%	0.84866074	146.03%	0.867239	16.37%	0.1345	-24.38%	0.14364624
800	304.83%	0.83984106	423.47%	0.79142381	187.32%	0.87406486	166.16%	0.94794	35.97%	0.3713	66.89%	0.82244766
850	252.93%	0.81844501	488.20%	0.83207968	186.73%	0.94277074	136.54%	0.666411	23.54%	0.5913	28.68%	0.83080763
900	212.07%	0.81462823	655.48%	0.929136	175.73%	0.87433537	-91.37%	0.699114	35.32%	0.7465	20.54%	0.85226042
950	182.75%	0.80494323	656.56%	0.96731464	222.61%	0.93258426	28.38%	0.334039	77.13%	0.9525	62.13%	0.97501973
1000	155.81%	0.80974661	558.51%	0.97995983	230.51%	0.97349349	47.67%	0.798637	44.75%	0.8615	26.42%	0.84805089
1050	138.64%	0.79806084	501.59%	0.98502929	209.99%	0.97771552	-17.89%	0.209213	4.32%	0.1391	36.44%	0.8695135
1100	115.94%	0.74198311	442.97%	0.96701945	195.90%	0.97394337	22.02%	0.36019	13.20%	0.4359	10.06%	0.17200101
1150	88.02%	0.65612083	321.16%	0.91144797	168.02%	0.96380061	66.46%	0.767669	29.25%	0.6151	43.88%	0.85120059
1200	66.88%	0.51612556	212.75%	0.77389374	151.13%	0.96263589	116.73%	0.920106	75.40%	0.8799	37.56%	0.93422606
1250	51.96%	0.3812386	125.12%	0.59558334	127.91%	0.97346949	128.54%	0.913887	102.28%	0.8686	66.22%	0.95599751
1300	44.62%	0.3189958	74.25%	0.58442739	118.71%	0.9879358	152.44%	0.965507	69.71%	0.9069	81.59%	0.90727397
1350	39.60%	0.27168299	33.74%	0.25893013	93.75%	0.94194508	125.28%	0.976384	80.86%	0.9931	46.37%	0.91851345
1400	42.31%	0.27210432	14.03%	0.06861129	69.04%	0.8070396	83.60%	0.958909	123.07%	0.9495	177.79%	0.92742048
1450	51.09%	0.28689294	18.18%	0.10455231	45.68%	0.5540801	22.36%	0.801111	30.59%	0.902	20.06%	0.80176974
1500	74.70%	0.39448766	43.83%	0.20644446	53.49%	0.54255526	11.63%	0.47432	10.49%	0.5824	10.63%	0.9774563
1550	94.90%	0.48965512	54.00%	0.20667568	73.99%	0.69718492	38.71%	0.882961	31.67%	0.8568	22.59%	0.94627124
1600	110.90%	0.56196066	98.36%	0.26145518	95.00%	0.76395166	52.99%	0.919715	32.76%	0.8094	31.35%	0.90561786
1650	127.45%	0.64947456	134.43%	0.40920131	107.22%	0.82535658	51.91%	0.932765	30.37%	0.8413	28.60%	0.88154368
1700	147.53%	0.73928878	134.09%	0.79998136	114.17%	0.88471947	42.91%	0.831897	16.66%	0.4788	62.91%	0.88352165
1750	169.57%	0.82332264	122.53%	0.91560774	120.62%	0.91734982	74.71%	0.906012	58.00%	0.8622	126.30%	0.95298997
1800	179.41%	0.86989136	127.17%	0.9294617	126.88%	0.93004944	97.65%	0.917214	61.61%	0.7998	109.39%	0.88814497
1850	178.78%	0.89230989	131.39%	0.94385133	131.28%	0.94563427	101.32%	0.954587	78.31%	0.9023	141.27%	0.91950002
1900	173.44%	0.91232425	136.83%	0.96543998	136.75%	0.96481374	95.54%	0.946655	65.64%	0.9633	86.03%	0.89381809
1950	169.15%	0.92027461	139.59%	0.97002998	139.55%	0.97002567	113.71%	0.956044	66.83%	0.8999	106.69%	0.92248018

Table 14 Percent increase from 2000 to 2030 and the goodness of fit for linier approximation used to derive that. This includes all 6 object sizes from 200km to 1950km.

## **Bibliography**

*Collisional Cascading: The limits of Population Growth in Low Earth Orbit*, Donald J. Kessler, NASA/Johnson Space Center, Houston, TX 77058, U.S.A.

UCS satellite database

[http://www.ucsusa.org/nuclear\\_weapons\\_and\\_global\\_security/space\\_weapons/technical\\_issues/ucs-satellite-database.html](http://www.ucsusa.org/nuclear_weapons_and_global_security/space_weapons/technical_issues/ucs-satellite-database.html)

Ordem2000

<http://orbitaldebris.jsc.nasa.gov/model/engrmodel.html>

[http://www.centennialofflight.gov/essay/Dictionary/GEO\\_ORBIT/DI146.html](http://www.centennialofflight.gov/essay/Dictionary/GEO_ORBIT/DI146.html)

Technical Report on Space Debris, United Nations, New York, 1999

[http://orbitaldebris.jsc.nasa.gov/library/UN\\_Report\\_on\\_Space\\_Debris99.pdf](http://orbitaldebris.jsc.nasa.gov/library/UN_Report_on_Space_Debris99.pdf)

<http://mathworld.wolfram.com/LeastSquaresFitting.html>

<http://spaceflight.nasa.gov/realdata/tracking/index.html>

<http://www.orbitaldebris.jsc.nasa.gov/faqs.html#12>

## **Acknowledgments**

David Belanger and the whole physics department at UCSC

NASA – for their wonderful ORDEM software and countless resources

Mom and Dad – the best proof readers and support group in the world